

December 2013

Volume 119

Issue 1932

£5.10

Electronics WORLD

THE ESSENTIAL ELECTRONICS ENGINEERING MAGAZINE

www.electronicsworld.co.uk

RENESAS



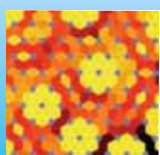
The RZ/A family: Next Generation HMI Solutions

Embedded MPUs with the 'Renesas Zenith' of Performance



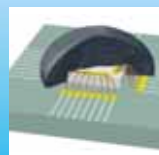
Technology

Semiconductor
spintronics breakthrough



R&D From China

Intelligent fault diagnosis
system for quality control



Packaging

New encapsulants for
microelectronics devices

Need a True Serial Data Expert?

Teledyne LeCroy Oscilloscopes



Efficient Serial Data Design and Debug

Leading Technology

- 8 Channel Solution
- HD4096 True 12-bit Technology:
 - 16x More Vertical Resolution,
 - Unmatched Measurement Precision
- 36 Digital Channel Mixed Signal Solution

Widest Range of Serial Data Tools

- CAN, LIN, FlexRay™
- MOST, BroadR-Reach, SENT, PSI5
- Manchester & NRZ Configurable Protocol Decode
- I²C, SPI, UART, Ethernet, USB, PCI-Express etc.

teledynelecroy.com/europe



TELEDYNE LECROY
Everywhere you look™

REGULARS

05

TREND

ELECTRONICS GIANTS LOCKED IN IP BATTLE

06

TECHNOLOGY

10

THE TROUBLE WITH RF...

DESIGNER!

by **Myk Dormer**

38

R&D FROM CHINA

AN INTELLIGENT FAULT DIAGNOSIS SYSTEM FOR
ELECTROMECHANICAL PRODUCTS' QUALITY
MONITORING AND CONTROL

44

T&M COLUMN

by **Reg Waller**

46

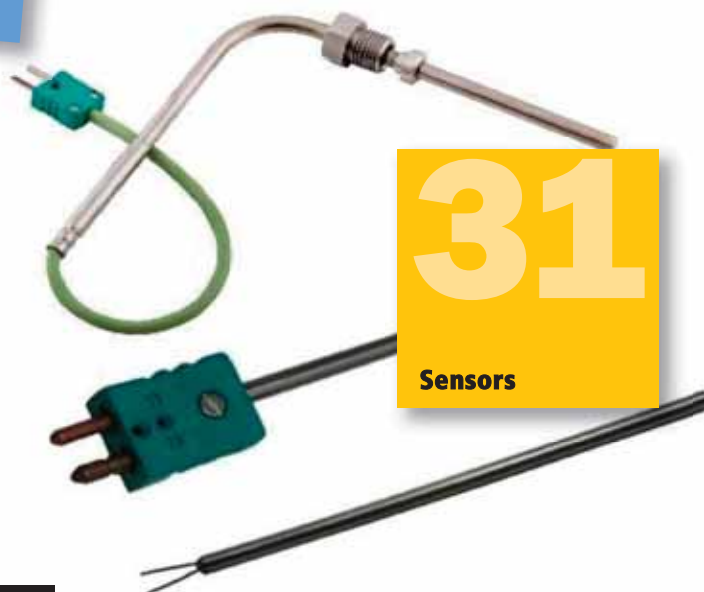
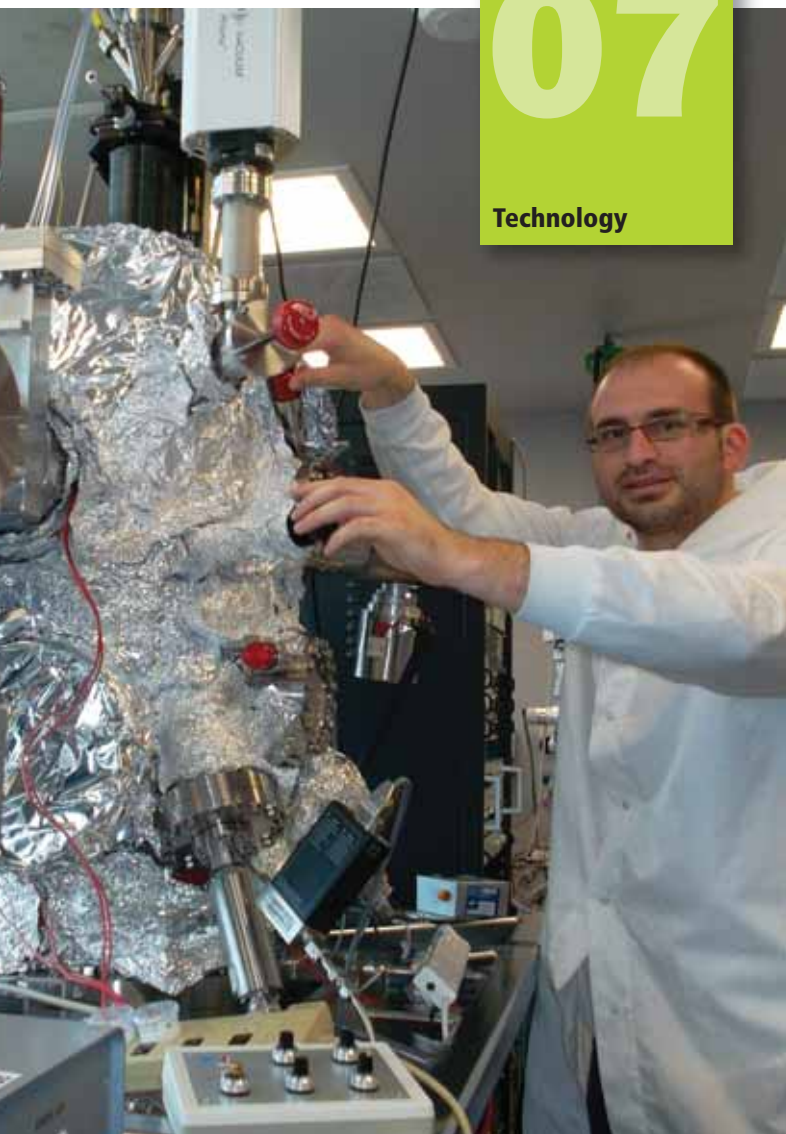
PRODUCTS

50

LAST NOTE

07

Technology



31

Sensors

FEATURES

12

OSCILLOSCOPE PARAMETERS – WAS EVERYTHING SAID ALREADY?

Thomas Rottach, Application Engineer at Rigol Technologies EU, discusses the important parameters of an oscilloscope

16

TIPS FOR MAKING THAT TOUGH THIRD-ORDER INTERCEPT MEASUREMENT

Nikhil Ayer, Product Marketing Manager for Test Systems at National Instruments, helps designers ensure measurement accuracy in their next high-linearity third-order intercept (IP3) measurements

18

A ROBUST HIGH-VOLTAGE SQUARE-WAVE SIGNAL GENERATOR WITH ADJUSTABLE FREQUENCY

By **Shaopeng Guan, Fuguo Dong, Changxin Nai** and **Wenyan Sun** from the Shandong Institute of Business and Technology in China

22

DESIGN OF A MICROCONTROLLER-BASED BODY HEIGHT MEASURING DEVICE

Professor Dogan Ibrahim of the Near East University in Cyprus describes the design of a microcontroller-based body height measuring device using ultrasonic techniques

26

A DISTRIBUTED IMAGE COMPRESSION ALGORITHM FOR ENVIRONMENTAL MONITORING APPLICATIONS

Aysegul Alaybeyoglu from the Computer Engineering department at the University of Celal Bayar in Manisa, Turkey, presents a distributed image compression algorithm for environmental monitoring applications in wireless multimedia sensor networks

31

HOW TO CHOOSE THE RIGHT TEMPERATURE SENSOR FOR YOUR PROJECT

Bernd Heim at Avnet Abacus explains the technology that lies behind various types of temperature sensors and how that determines their performance

34

HIGHLY RELIABLE ENCAPSULANTS FOR MICROELECTRONICS

Newly-developed encapsulants help protect sensors, actuators and semiconductors from the harshness of the environments they may be placed in. By **Dr Tobias Königer**, Product Manager at DELO Industrial Adhesives

Disclaimer: We work hard to ensure that the information presented in Electronics World is accurate. However, the publisher will not take responsibility for any injury or loss of earnings that may result from applying information presented in the magazine. It is your responsibility to familiarise yourself with the laws relating to dealing with your customers and suppliers, and with safety practices relating to working with electrical/electronic circuitry – particularly as regards electric shock, fire hazards and explosions.

Unrivalled Performance, Flexibility and Value for Automated Test



NI PXI hardware, combined with NI LabVIEW system design software, delivers increased performance, flexibility and value. Using this combination of modular hardware and productive software, engineers have dramatically reduced costs, realised faster test execution, improved throughput and increased scalability. With more than 500 PXI products, over 200 global locations and 700+ Alliance Partners, NI offers the only complete solution for your ever-changing automated test needs.

LabVIEW helps you program the way you think—graphically, while simplifying your approach with built-in analysis and unmatched hardware integration.



>> Accelerate your productivity at ni.com/automated-test-platform

01635 517300 | uk.ni.com

See what you missed at NI Days 2013: download presentations, view videos & pre-register for 2014 at uk.ni.com/nidays

Follow us on



Search **niukie**



ELECTRONICS GIANTS

LOCKED IN BATTLE

The on-going infringement battle between electronics giants Apple and Samsung over touchscreen smartphones and tablets is one of the **biggest IP news stories of recent years. It is also one of the most complicated.**

Infringement proceedings involving the two have taken place in ten countries, concerning registered designs, trademarks and patents. Some of the proceedings were brought by Apple, some by Samsung.

Further complication is added by the infringement cases brought by Samsung on Standards Essential Patents (SEPs), concerning those patents with subject matter incorporated into technical standards such as 3G and WiFi. Holders of SEPs are obliged to offer fair, reasonable and non-discriminatory (FRAND) licences to those who implement technology using the standard. In the US, the Obama administration recently vetoed an injunction obtained by Samsung preventing the sale of some older Apple devices, on the basis that it hadn't offered Apple a FRAND licence.

Samsung's successes include an important non-infringement decision in the UK for the look of its tablets and the SEP infringement cases. Meanwhile, Apple won over \$1bn in damages and has been successful in obtaining injunctions preventing the sale of certain Samsung devices in Germany, the US, Australia and the Netherlands.

Of course, it's not quite that black and white. Samsung has emerged as the main rival to Apple in the smartphone and tablet market, and outperforms considerably in terms of units shipped. Although involved in infringement lawsuits, it seems that \$1bn may be a reasonable price to pay for Samsung in maintaining and growing its market share. One might think that Apple has prevailed because it held a greater quantity of patents.

The nature of the two companies is quite different: Samsung's product range is broad, encompassing smart phones, televisions, cameras, laptops, fridges, vacuum cleaners, washing machines and more – encompassing a broad patent portfolio, over hundreds of different technology areas.

Apple has a comparatively tiny product range, consisting of smartphones, MP3 players, tablets and computers. Each category has only a few products, and just two or three new devices are released each year.

Despite the numerical disadvantage, Apple's portfolio was clearly focused on specific technological areas, such as communications

Samsung has emerged as the main rival to Apple in the smartphone and tablet market, and outperforms considerably in terms of units shipped

protocols and user interface icons. Samsung's far larger, but broader, portfolio gave it little ammunition to fire back at Apple, and it resorted to infringement cases involving SEPs.

Notwithstanding these complexities, there are several lessons here that have implications wider than the machinations of huge multinational companies, and that are relevant to SMEs trying to protect their investment in R&D.

Firstly, it appears Apple was very careful to avoid infringing rivals' patents whilst developing its devices. Considering the size of Samsung's portfolio, this was quite a feat. Money spent on researching rival patent holdings before designing the product put Apple in a very strong position in the ensuing infringement proceedings.

Secondly, Apple's focus on protecting features of the touchscreen interfaces, such as pinch-to-zoom, rather than deep behind-the-scenes technology, made infringement easier to prove. It also meant that users expected these features, making it much harder for competitors to design around them.

The dispute also raises questions about how later entrants into a market can catch up with the market leader. It's not just Samsung that has struggled with this problem; HTC, Motorola and Nokia have all had to deal with the Apple's rise. Broadly, they have all opted to produce touchscreen phones with a similar look and functionality to the iPhone.

One aspect of the solution is accurately assessing the IP holdings of your competitors. Taking into account the detailed subject matter protected by their patents is vital. Another is ensuring your patents protect innovative and exciting features and products, increasing your all-important bargaining power if there are issues of infringement or negotiations over licencing. In these situations, you don't want to look in the cupboard and find it bare.

Finally, the conclusion that is both the most obvious to draw and the most difficult to act upon: it pays to predict the trend early, innovate early and patent early. Apple led the smartphone boom; Samsung has done well to catch up. The continuing challenge is predicting the next boom: Wearable technology? 3D printing? Without a crystal ball, it's hard to know. What we do know is that, when it comes around, clever management of IP strategy will be key.

Ian Robinson is Head of Electronics at Appleyard Lees, European patent and trademark attorneys (www.appleyard-lees.com)

EDITOR: Svetlana Josifovska
+44 (0)1732 883392
Email: svetlanaj@sjpbusinessmedia.com

DESIGN: Tania King
Email: taniak@sjpbusinessmedia.com

SALES: John Steward
Tel: +44 (0)20 7933 8974
Email: johns@sjpbusinessmedia.com

PUBLISHER: Wayne Darroch

ISSN: 1365-4675
PRINTER: Buxton Press

SUBSCRIPTIONS:
Tel/Fax +44 (0)1635 879361/868594
Email: electronicsworld@circdata.com
SUBSCRIPTION RATES:
1 year: £56 (UK); £81 (worldwide)

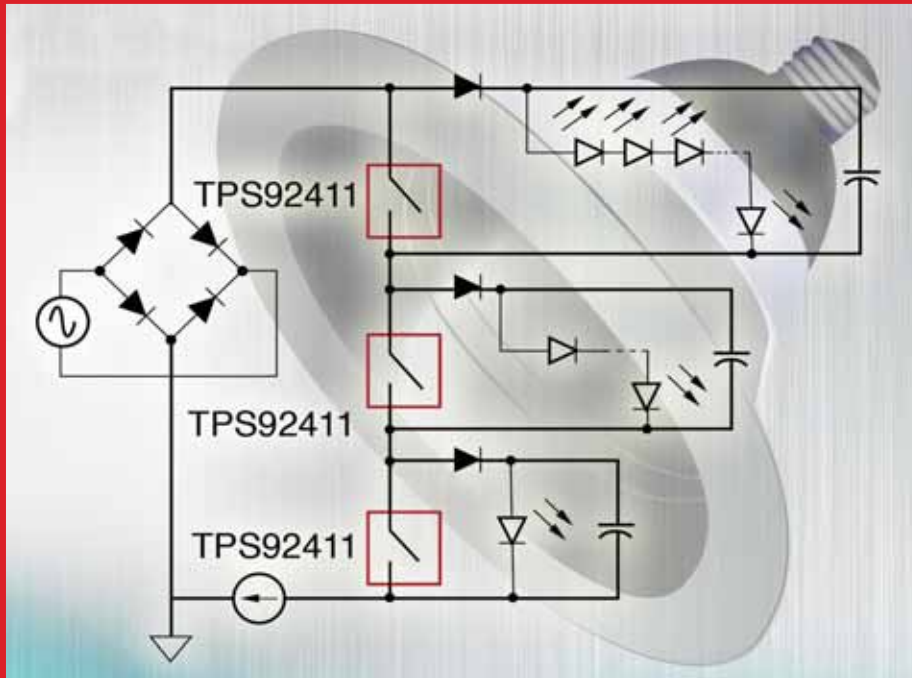


Follow us on Twitter
@electrowo



Join us on LinkedIn
<http://linkd.in/xH2HNx>

FLOATING SWITCH ARCHITECTURE FROM TI TRANSFORMS OFFLINE LED DRIVE DESIGN



TI's TPS92411 floating MOSFET switch

Texas Instruments (TI) introduced the industry's first floating switch architecture that simplifies the offline linear drive of LEDs in lamps, downlights and fixtures. The AC switched matrix technique features TI's TPS92411 floating MOSFET switch and is an innovative approach to producing low-ripple LED drive

current without magnetic components. The architecture allows compatibility with legacy wall dimmers and delivers high power factor and low total harmonic distortion (THD).

Flyback, buck and boost converters are common switch-mode power supply (SMPS) topologies in LED lamps. These

circuits operate at high frequencies and require inductive components to turn mains AC current into the constant DC current necessary to drive LEDs. Selection of inductors and transformers for power transfer is complicated, often requiring expensive custom components. In addition, an electromagnetic

interference (EMI) filter consisting of up to ten passive components is often needed to prevent the SMPS circuit from harming other electronic equipment. If phase dimming is required, multiple design iterations may be necessary to optimize dimmer compatibility and prevent LED flicker.

The floating switch architecture with TI's TPS92411 overcomes these challenges and it requires no inductive components for power transfer, eliminating cost and bulk and simplifying design.

The TPS92411 joins TI's diverse LED driver portfolio that includes the TPS92075, LM3447 and LM3445. Its main features include a 100V, 2-Ohm floating MOSFET switch with 350mA current capability, power factor greater than 0.95, total harmonic distortion (THD) of less than 15%, and others.

Arm Targets Automotive And Industrial Control Markets With New Architecture

ARM has disclosed technical details of its new ARMv8-R architecture for real-time embedded processors aimed at automotive and other integrated safety and control applications.

Key innovation within the ARMv8-R architecture is the introduction of a 'bare metal' Hypervisor mode, which enables programmers to combine different operating systems (OS), applications and real-time tasks on a single processor whilst ensuring strict isolation between them. This will help with software consolidation and re-use, which should accelerate time-to-market and reduce development costs. In addition, the ARMv8-R architecture will

enable overall improvements in software quality and will support increasingly sophisticated embedded programming techniques such as model-based automated code generation.

The architecture also permits coexistence of both virtual memory and protected memory systems on the same processor, enabling an operating system using memory management, such as Linux, to be integrated with an RTOS. Other features include improved memory protection scheme, which substantially reduces context switching time; ARM NEON advanced SIMD instructions for significantly improved

image signal processing tasks; and the functionality to detect corruption of program code or data via instructions such as CRC (Cyclic Redundancy Check).

ARM is now working on a design ecosystem to support the new features, including the DS-5 ARM tools and Fast Models. Timed models, automotive simulation system level tools and mechanical and electronic modelling tools are being developed by EDA partners in advance of silicon.

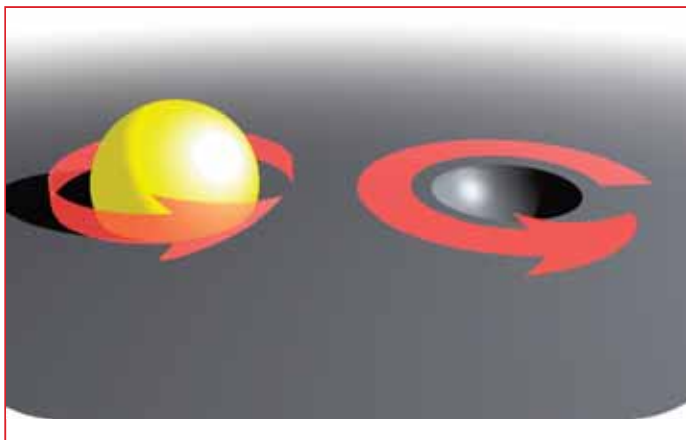
Ecosystem support for the ARMv8-R architecture is anticipated in a number of OS products including INTEGRITY from Green Hills Software, Nucleus from

Mentor Graphics and T-Kernel from eSOL. These integrated hardware and software solutions will be capable of supporting stringent automotive and industrial interoperability and safety standards, including AUTOSAR, ISO 26262 and IEC 61508.

The ARMv8-R architecture specification will be available to partners under license; support for the ARMv8-R architecture will be available to lead partners in the latter part of next year.

ARM processors which implement the new architecture are in development and details of these will be disclosed at a later date.

Rare Earth Nitrides: The New Kids On The Block For Semiconductor Spintronics



Electrons and holes share the same spin orientation

A team of researchers from New Zealand have shown a new class of materials, called rare-earth nitrides (RENs), that will pave the way to new type of electronics through semiconductor spintronics. Dr Franck Natali and his team from the Victoria University of Wellington (VUW) now plan to develop the first spintronic devices based on RENs, including magnetic tunnel junctions (for data storage devices), spin LEDs (for communications) and spin transistors (for logic operations).

Until recently RENs were considered exotic materials, studied by a few theorists. However, a series of breakthrough discoveries suggest that RENs hold promise in electronic applications, or semiconductor spintronics specifically.

Spintronics is the extended electronics that takes advantage of not only the charge, but also the intrinsic magnetic properties of the electron – its spin. Spintronics is already at the heart of commercial magnetic metal-based devices such as read heads in large capacity hard disk drives.

One of the challenges is to extend practical spintronics into the realm of semiconductors to develop devices that can outclass existing electronics regarding speed and power consumption.

“In the past 15 years many researchers have focused on the

spintronics promise of diluted magnetic semiconductors (DMS), which are formed by a moderate concentration of magnetic atoms incorporated into semiconductors,” said Dr Natali. “We think that intrinsic ferromagnetic semiconductors such as the RENs can offer an interesting alternative.”

The rare earths comprise the elements with atomic numbers from 57 (Lanthanum) to 71 (Lutetium), the elements with the largest spin and orbital moments. Their nitrides have been studied for nearly 50 years, but with

disagreements concerning even such fundamentals as their conducting state, metal or semiconductor. Recent advances in thin film fabrication with ultra-high vacuum based growth technology have already revealed most as ferromagnetic and semiconductor, a very rare combination.

The Materials for Spintronics group at VUW have led the way by synthesizing high quality thin-films of half of the fourteen RENs. The series includes members with small and huge coercive fields and promising complementary electronic properties, offering potential for memory element and electronic applications.

Like the DMS, the ferromagnetic state of RENs is so far only well below room temperature, but unlike the DMS they permit doping control of the carrier concentration and charge carrier sign without affecting the magnetic properties. Furthermore electrons and holes share the same spin orientation; both are of spin up character (see figure); they will support the formation of bipolar diodes and transistors with only up-spin conducting channels. The single-spin channel of GdN has already

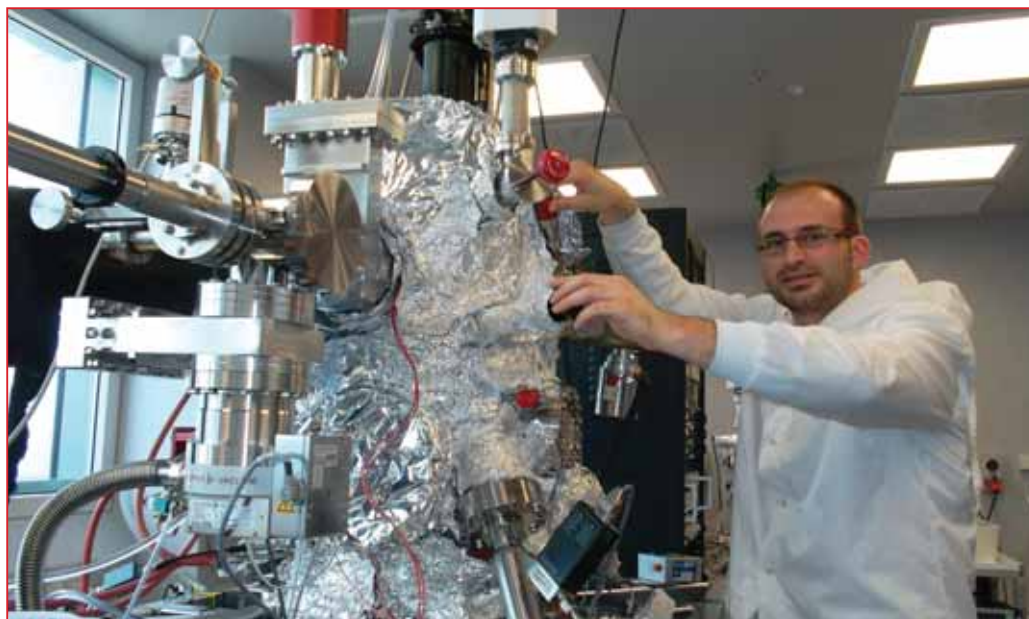
been exploited in a spin filter.

The technological potential of the RENs is enhanced by epitaxy-compatibility with group III-nitrides (GaN, AlN, InN), the technologically important family for the fabrication of visible LEDs and high power transistors. Their narrow band gap complements the wide band gap group-III nitrides, so that a heterojunction involving the two semiconductors might have very attractive properties for multi-wavelength photonic devices. A prototype combining both technologies has already been demonstrated, by the use of GdN quantum dots to enhance the efficiency of GaN tunnel junctions.

There has been no more than a start at investigating these REN compounds, but the prospect of electronic and spintronics applications can be one of the driving forces for their development.

The team's project has now received a further financial boost from the Royal Society of New Zealand to cover the next three years in collaboration with the CRHEA-CNRS (France). “That will move us closer to developing and constructing spintronics devices,” said Dr Natali.

Dr Franck Natali of the Victoria University of Wellington (VUW) in New Zealand



THE RZ/A AS USED IN AN APPLICATION EXAMPLE

By Robert Kalman, Product Marketing Manager, Industrial Communications Business Group
Renesas Electronics Europe GmbH

The Human Machine Interface market for driving medium to large TFT panels is expanding at an enormous pace. Before Apple took the world by storm, there was the constant dismissive discussion in technical circles about "who would want to have a colour screen on their telephone?"

We were all proved wrong: in addition to phones, the number of coffee machines, refrigerators, vending machines and the likes that are fitted with a TFT panel is set to rise significantly over the next few years.

SO WHAT DO YOU NEED FOR YOUR APPLICATION?

Most TFT panels today use a digital RGB interface, whether that be RGB888 or RGB565. The RGB value is a standard whereby the colours red, green and blue of each pixel are represented by the corresponding number of bits. So for 888 each is given a full 8 bits of data (giving 24 bits per pixel), whereas in 565 the red and blue are represented by 5 bits and the green by 6 bits (giving 16 bits per pixel). Alternatively, instead of a standard digital interface a screen could be using an LVDS connector, as is increasingly becoming the standard with larger screens. As such, the RGB signals are transferred over a differential signal, but the format of the data is still the same. So to start with, you need a device that supports the generation of an RGB signal and/or an LVDS interface.

Second to that, the RGB data has to come from a frame buffer, which is typically stored in RAM. This frame buffer is a bitmap image stored in the desired format. Thus, a screen size of WVGA for example (which is 480x800) will need for an RGB888 image just over 1MB of RAM to store the image ($480 \times 800 \times 24 \text{ bits} = 1.125\text{MB}$).

In addition to this frame buffer containing the current picture being displayed on the screen, a typical application will have a "back buffer" that contains the next picture to be driven to the screen. This way, the CPU can manipulate the next picture without the user seeing a half-manipulated picture flickering on the screen before the CPU is finished. This system of double buffering is very

common and gives an overall higher quality of HMI, but also means that the WVGA screen needs a further 1.125MB of RAM to store the buffer.

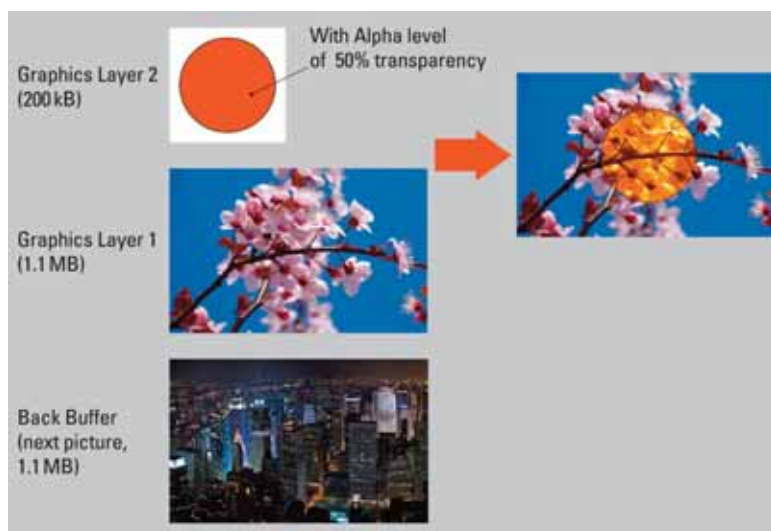
In a typical HMI application it is not always necessary to manipulate the whole screen. For example, if an icon or button is pressed, it might animate, glow, rotate or somehow react prior to the action being taken. In this case, what an HMI designer would do would be to define a different layer of the picture. There would be a background layer that would be unchanged and the icon or button would be a foreground layer, which would then be animated. However, this obviously also needs additional RAM, not a full screen but "some" more. It depends on the size of the image, but with a 200 x 200 pixel button we would need an additional 100k of RAM. What is also required here is the ability to blend all these different layers with one another, and perhaps apply a level of transparency to some of those pictures. This can be done in software if the CPU is fast enough, or in hardware if it is available.

A reasonable HMI application can use in the region of 3MB as frame data for a WVGA screen size. If the code is running on RAM too, as is the case with most processors, then a further 0.5MB of code is needed. Thus the starting point for a WVGA screen should be to look for a system with a minimum of 3.5MB of RAM.

Of course, the speed of access to the RAM is also very important. As you will have likely just realised, the RAM here is being written to and read from by several different sources concurrently. For example, the front buffer (the original image data) will be read by the IP block to drive the data to the screen. At the same time, the back buffer will be updated by the CPU or by a DMA transfer of a different image. At the same time as this, the CPU may be manipulating the aforementioned icon, and reading its own code from the RAM. This puts a lot of pressure on the bandwidth of the bus to the RAM. This bus is very often the bottleneck in the application, so a good system of bus architecture is required to mitigate the risk of overloading the bus and of the user seeing some half-finished images, or worse still a non-functional GUI.

Special attention should also be paid to the performance of the CPU. A system delivering 24 frames per second to the screen will need to manipulate and create data (in our example of a WVGA screen) of over 24MB per second. This can be done entirely in software, or in some parts in hardware, but whatever happens the CPU must be fast enough to cover these requirements.

As we are now clearly talking about a processor solution, which is likely not going to have any flash memory on chip, the next requirement is that of a connection to external flash memory. The typical method for today is to use an external parallel NOR flash to store the code and then during boot mode to transfer this code into the RAM to support fast execution. Newer devices, however, support other memory technology to allow system architects to reduce system cost without having the overhead of an "expensive" NOR flash on the PCB.



Most of these applications typically do more than just drive a screen. They need to be connected to the rest of the system too. Automotive applications are typically connected to the CAN or MOST bus. Industrial and consumer devices today generally require Ethernet and USB connections. These connections also mean that the most suitable product will have to not only incorporate the hardware IP, but also have sufficient performance to manage their operation and sufficient code space to support their stacks.

SO HOW ABOUT THE RZ/A?

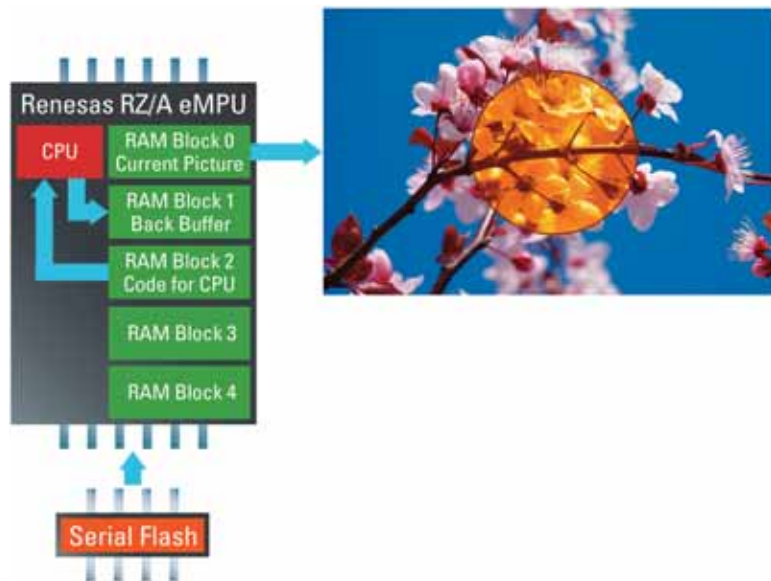
The RZ/A family is an ARM Cortex A9 based embedded MPU solution that brings a great many advantages to the HMI application space. The RZ/A features up to 10MB of embedded SRAM on chip, which makes it the largest embedded RAM in the market. There are 3 variations in the family. The RZ/A1H which includes the full 10MB of RAM, the RZ/A1M which has just 5MB of RAM, and the RZ/A1L which includes the lowest 3MB of RAM.

So from the discussion above, where we calculated that the HMI application would need approximately 3.5MB of RAM, the RZ/A1M looks ideally suited to meet these requirements. It is of course possible to find several other solutions on the market that will use external RAM, whether it be DDR or SDRAM, to cover this size of memory but the RZ/A family is the only product that the author is aware of that can offer such a high level of internal RAM.

The RZ/A1H gives the system designer room to increase the screen size and also to decrease the screen size depending on requirements, and create a cost-optimised version for smaller resolution products.

The 400MHz CPU performance is more than enough to run a simple HMI application and maintain communication through whichever protocol the system dictates, because all versions of the RZ/A family include CAN (up to 5 channels) Ethernet and USB (up to 2 channels).

In fact, the 400MHz CPU is more than enough due to two unique features of the RZ/A. The first feature is the VDC. The video display controller from Renesas supports in hardware many of the functions required for creating the final screen image. The VDC will support up to 4 different graphics layers, two of which can be inputs from an external camera. It will also support alpha blending hardware. Alpha blending is a process whereby each pixel is allocated an additional 8-bit alpha value. This alpha value determines the transparency of the pixel, such that it can be overlaid on top of another pixel to create the resulting image. The VDC also supports chroma-key operation, the most well-known use of which is in "green screen" videography, where a

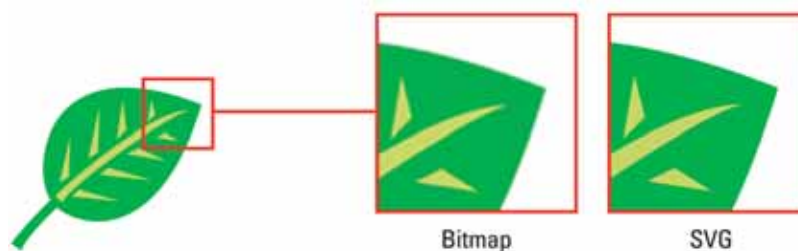


particular colour is defined as transparent so that an object can be overlaid again on another picture. In some systems all of this would be done in software, but the RZ/A does it in hardware, thus the 400MHz in reality equates to a much higher equivalent performance. The VDC also supports the RGB digital connection to a TFT screen as well as the LVDS.

The second performance factor of the RZ/A family that boosts the CPU performance is the removal of the bus bandwidth problem we saw earlier. A quad-core terahertz processor is only as fast as it can get the data. When that data is all stored in a single RAM block to be accessed over a single bus, this is bound to slow down the core. The RZ/A, in contrast, has 5 separate RAM banks. Each bank is connected to its own dedicated 128-bit wide bus, such that it is actually possible to both write to the back buffer, read from the front buffer, manipulate an icon and complete a DMA transfer all whilst running code from the internal RAM. This is a significant performance boost.

Of course, we mentioned earlier that a connection to external flash memory is also needed, and the RZ/A supports all the normal connections to non-volatile memory such as NOR, NAND, SDIO, MMC etc. However, it also has a special SPI Multi-I/O serial flash connection, which supports the new quad SPI protocol. This QSPI can achieve similar or better performance figures to those of parallel flash while providing the economic advantages of serial flash, as well as saving pins on the microprocessor and reducing PCB size.

www.renesas.eu





Designer!

MYK DORMER IS A SENIOR RF DESIGN ENGINEER AT RADIOMETRIX LTD
WWW.RADIOMETRIX.COM

November 5th was the birthday of a hero of mine: Raymond Loewy. For those of you unfamiliar with this name (or who didn't notice the rather fetching logo used by Google that Tuesday), Loewy was a giant in the field of industrial design, responsible for the appearance of many of the iconic images and forms of the nineteen thirties, forties and fifties, such as the futuristic Pennsylvania Railway's streamlined steam locomotives, the 1946 Lincoln Continental, the first Coca-Cola can, the Hillman Minx, the livery used on Air Force One and so on. His later work included such varied things as corporate logos (Shell, Exxon, Chubb and Spar, to name a few) and the interior designs of the Concorde (Air France version) and NASA's Skylab.

It can be fairly argued that Loewy is one of the fathers of industrial design as we currently understand it. Unfortunately, the genius and vision of such designers has led to a far less desirable subsequent result: the deliberate, formal separation of "design" and "engineering".

Superficially this might not seem to be a problem. Design can be seen as a creative, imaginative, artistic activity, dealing with shapes, forms, textures and colours. Engineering on the other hand is seen as mathematical, methodical and exacting, concerned with obscure and invisible inner workings. Regrettably, like many superficial views of complex subjects, this is also profoundly misleading.

This flawed model views a "design" as an artistically-inspired abstract form conceived of in isolation by the designer, into which the subordinate engineers subsequently pour the "magic fluid" of functional, physical

reality. While such a vision may be philosophically satisfying, it fails to appreciate that, while the appearance and form of a design are important, they are only a part of an overall whole, which is ultimately governed by engineering principles. This is not to say that overall form has no place in a design (featureless grey boxes are aesthetically unsatisfying, commercially undesirable and ergonomically deficient) but it cannot be allowed to supplant good engineering practice. I can offer an example:

As a younger, brighter-eyed engineer I once worked for a company that designed very small underwater ROVs (miniature unmanned submarines, equipped with cameras and powerful lights). The engineering team was large (over a dozen) and multi-disciplinary, including mechanical, electronic and marine engineers. About four months into the project we had converged on a fairly satisfactory design: thrusters that worked, good control and video sub-systems, a safe and reliable battery assembly, all packaged into a hull the size and (approximate) shape of a fire extinguisher.

At this point our higher managers decreed that the project needed "design" and called in a then well-known design consultancy. I will forbear to mention their name, but suffice to say they ticked every box in the engineer's list of why we don't like artists. They acted, and were allowed to act, as if they came from a higher plane of existence. They posed, postured and held long, long meetings. They excluded the existing engineering team from all significant decisions and treated the physical constraints of mechanical, electrical and hydrodynamic design as if they were minor, unwelcome intrusions into their sphere of aesthetic perfection.

They came up with a new "less militaristic, more organic" shape. We engineers then dutifully re-cast (and compromised) our component parts and shoehorned them into the new hull. The result certainly didn't look like any conventional underwater craft (manned or ROV) and, in so much it was, I suppose, "innovative".

Unfortunately, as they found out on the grand day of unveiling and testing, it also didn't work. Its in-water drag coefficient was huge, it lacked any measure of directional control and, while it could creep sluggishly along the surface, once underwater it was totally unstable.

We never saw the "designers" again. After a few more fruitless test runs we quietly returned to the original configuration, eventually refining the original parts to fit into a roughly tear-drop shaped casing, with a passing resemblance to a rather plump goldfish. Hydrodynamically this worked well, but we had already lost six irreplaceable months and the project eventually foundered.

I think there is a lesson in this. Industrial design and engineering must operate synchronously: the physical constraints and component dimensions must influence the overall artistic form, in the same way that the conceived form should influence the choice and disposition of those component parts. This idea isn't even new: it is found in the theories of the Bauhaus art/design movement of the nineteen twenties, and expressed in the "form follows function" credo followed by the Modernists.

Separating the disciplines of "design" and "engineering" is not only inefficient and socially divisive, but is also terribly wasteful of the inherent well of creativity and ideas that is found within all of us – even those of us who are engineers. ●



NRPL Group seeks out XJTAG Boundary Scan for radar

“NRPL Group specialises in civil radar, serving air-traffic control authorities in several countries. Engineers place high importance on testing to ensure the best possible quality and – ultimately – safety. XJTAG boundary scan is an important part of their test strategy, offering powerful features, flexibility and high-quality support at a competitive price.”

NRPL Group is a Finland-based specialist in radar for air-traffic control, and has group companies in Czech Republic and Russia. Its products include Primary Surveillance Radar (PSR), Monopulse Secondary Surveillance Radar (MSSR) and advanced Automatic Dependent Surveillance-Broadcast (ADS-B) solutions, as well as radar data processing and distribution systems, air traffic control and management systems, voice and data recorders. The company also supplies associated systems and sub-units such as radio equipment and signal and data processing systems.

Rigorous testing of all boards and systems is extremely important, from early design verification through prototyping and testing production units. “Radar is essential to the safe, efficient operation of an airport. It is absolutely vital for us to ensure total dependability of all systems before shipping to our customers,” comments Reidar Gjerstad, Senior System Engineer at NRPL’s main Finnish site at Vantaa. His team is using boundary scan as part of the strategy for testing prototype and production radar-controller boards, and XJTAG is the chosen solution.

“Writing tests using XJTAG and executing them via the boundary scan port is faster than other methods for testing our boards,” explains Reidar Gjerstad. “XJTAG really helps to speed up our prototyping activities by allowing us to assess any new digital circuitry within minutes.”

Another key benefit of using XJTAG is that engineers can begin

preparing tests for a board before the prototype hardware is built, enabling faster development. “We can start writing tests straight after the netlist is generated, which means we can be ready to test the first prototypes as soon as they arrive,” adds Reidar Gjerstad. “Also, writing test scripts is easy, using the high-level XJEase language, and

many scripts for standard non-JTAG devices are already available from XJTAG or can be easily modified from existing code.”

The XJTAG system also provides the flexibility to test analogue circuitry within the boundary scan test environment. NRPL is taking advantage of this to test various ports and check power supply voltages. “By building a simple adapter containing a DAC or ADC, we can use XJTAG to generate analogue test voltages or check the voltage on various pins such as power supply outputs and analogue ports.”

XJTAG provides support for customers seeking to exploit the

system’s analogue-test capabilities, and a detailed application note is available with sample code for testing a video DAC port. This note describes the test connector and typical techniques for generating or capturing analogue voltages using XJTAG.

“The support provided for XJTAG is wide ranging and of high quality, which has helped us get the best from the system and speed up our product development and test engineering activities,” continues Reidar Gjerstad. “Overall XJTAG gives great power and flexibility at a competitive price, and it is clear that a great deal of work has gone into making the features as accessible and as easy to use as possible.”

opinion

Reidar Gjerstad
Senior System Engineer
NRPL Group Oy

“XJTAG really helps to speed up our prototyping activities. We can start writing tests straight after the netlist is generated, which means we can be ready to test the first prototypes as soon as they arrive. Writing test scripts is easy, using the high-level XJEase language, and many scripts for standard non-JTAG devices are already available.”

“The support provided for XJTAG is wide ranging and of high quality. Overall XJTAG gives great power and flexibility at a competitive price. A great deal of work has gone into making the features as accessible and as easy to use as possible.”

**Data
Bank**



Company
History of
business
Main
products

NRPL Group Oy, HQ Finland
Manufacturer and supplier of
ATC surveillance equipment
PSR, MSSR Mode S and
ADS-B solutions, radar data
processing and distribution
systems, air traffic control and
management systems, voice
and data recorders

Customers
Location
Incorporated
Web site

Defense & Space
Vantaa, Finland. Group companies
in Finland, Czech Rep., Russia
1992
www.nrpl.aero

OSCILLOSCOPE PARAMETERS – WAS EVERYTHING SAID ALREADY?

THOMAS ROTTACH, APPLICATION ENGINEER AT RIGOL TECHNOLOGIES EU, DISCUSSES THE NOT-TO-FORGET ASPECTS OF AN OSCILLOSCOPE



Many articles have discussed the important parameters of an oscilloscope, such as bandwidth, sample rate and big data memory, but they still remain crucial when choosing an oscilloscope. It is only too easy to lose sight of the basics and become unaware of any new developments, so here is a reminder.

Oscilloscope Basics

Bandwidth determines the oscilloscope's fundamental ability to measure a signal; it is the frequency of the “-3dB point” of a sine-wave signal of a particular amplitude, so the key aspects to be aware of are:

- Amplitude errors at the frequency limit (~30% @ 3dB cut-off frequency);
 - Harmonics of the non-sine wave signals (FFT analysis).
- Out of these we can generate the following rules of thumb:
- At least the 5th harmonic should be covered by the scope's bandwidth;
 - The amplitude error @ freq = bandwidth/5 is roughly 3%.

If we keep these ‘rules’ in mind, then normally there won't be any further issues. But, just in case, let's go through an example.

Example

In our example, the maximum frequency to be measured is no more than 10MHz than the clock signal. The 5th harmonic of 10MHz = 50MHz, fitting into the 50MHz/5 = 10MHz frequency parameter, with a 3% amplitude error at 10MHz.

To be on the safe side, this should be doubled, which comes to 100MHz – the bandwidth of the new scope.

Typically, however, measurement of the rise and fall times of the clock signal is very common. In our example, the chosen 100MHz oscilloscope has a rise time of 3.5ns (clock signals normally have rise times typically of 2ns – TTL technology, or smaller). If this rise time is to be measured with a 100MHz scope, we will see a rise time of around 4ns on the scope screen, which effectively is an error of 100%.

Mathematically speaking:

$$\text{display rise time} = \sqrt{\text{inherent scope rise time}^2 + \text{signal rise time}^2}$$

so at which point was the mistake made?

The problem is that another well-known relation was not considered, and this is: ‘The steeper the rising edge, the more harmonics have to be taken into account’. The additional formula (valid for ‘10%-90% rise time’) to calculate the minimum required bandwidth is therefore:

$$\text{Bandwidth or Frequency} = \frac{0.35}{\text{Rise time}}$$

If we now change the rise time to 2ns for our clock signal, the minimum bandwidth we get is 175MHz. The next best standard oscilloscope bandwidth is 200MHz (with inherent system rise-time of 1.75ns). Applying the first formula again, the displayed rise time is 2.65ns. This is still a measurement error of roughly 33%, so the recommendation is to triple the calculated bandwidth, which brings us to the 500MHz bandwidth of a mid-class scope.

If probes are used with the scope, their bandwidth needs to be taken into account too. So, the bandwidth of the whole system is calculated as follows:

$$\frac{1}{\text{System Bandwidth}} = \sqrt{\left(\frac{1}{\text{Probe Bandwidth}}\right)^2 + \left(\frac{1}{\text{Oscilloscope bandwidth}}\right)^2}$$

Out of this we can generate another rule of thumb: *The bandwidth of the probe should be minimum 1.5-times bigger than the bandwidth of the scope.* (The standard probes delivered with Rigol Oscilloscopes fulfill this rule.)

The resulting system bandwidth is the most relevant factor to be considered every step of the way.

Sampling Rate

Sampling rate is a parameter related to bandwidth. The Nyquist/Shannon Theorem describes the relationship between the two, which in a nutshell is: *The sampling rate has to be a minimum of twice the highest, sampled, frequency component of the sampled signal.*

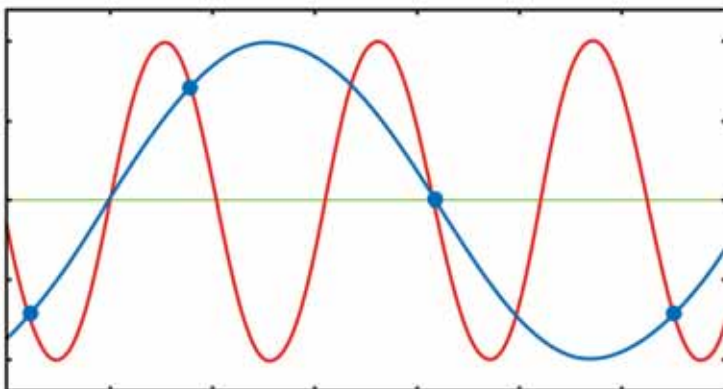


Figure 1: The signal of choice (in red) and its sin(x)/x function (in blue)

If we use this rule and extend the factor to 2.5, then an oscilloscope with a 200MHz bandwidth should work fine with a sample rate of 'only' 500MS/s.

So, what's the reason for oscilloscope manufacturers using more expensive A/D converter technologies with sampling rates of, say, 2GS/s in their scopes?

Briefly, the main reasons are: preserve signal integrity as much as possible, and be able to acquire as much signal detail as possible.

Going back to the Nyquist/Shannon theorem, we can easily see what might happen if this rule is broken. In Figure 1 the original signal is shown as the red curve, which is under-sampled. To display the result, the sampled points are normally interpolated with a $\sin x/x$ function (blue curve). The result is also a sine wave, but with a lower frequency than the original one. This effect is called 'aliasing'.

The green area in Figure 2 does not fulfill the Nyquist's requirements. Additionally, the amplitudes of the frequencies within it are big enough at the ADC's input that aliasing occurs and the 'transferred' frequencies affect the measured signal inside the pass-band ($f < f_{3dB\ BW}$).

There are two possible ways to resolve this problem, or at least reduce it to a negligible level. One is to use a band filter

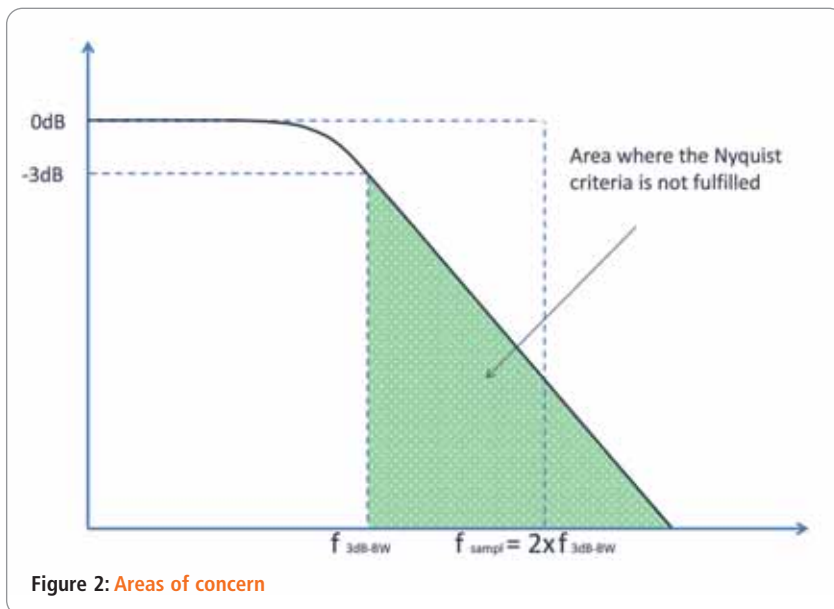


Figure 2: Areas of concern

with a sharper edge; and the other is to increase the sampling frequency, which means shifting the frequency (f_{sample}) right.

Analysing Solutions

Using a very sharp falling-edge filter will offer the advantage of the sampling frequency corresponding to the Nyquist theorem at a specified minimum. The ideal filter

OSCILLOSCOPES

SPECTRUM ANALYZERS

ARB. WAVEFORM GENERATORS

DC POWER SUPPLIES

MULTIMETERS

NEW! DIGITAL & MIXED SIGNAL OSCILLOSCOPE SERIES

Best Price:
from **€450,-**
plus VAT

Best Price:
from **€2,475,-**
plus VAT

DS1000Z

4 Channel Scope for 2 Channel Price!

- 70 to 100 MHz Bandwidth
- Standard memory depth up to 12 Mpts, optional up to 24 Mpts
- 1 GSa/s. max. Sample Rate

MSO4000

Based on the successful DS4000 series:

- 100 MHz to 500 MHz Bandwidth, 2 or 4 channels, 4 GSa/s, 140 Mpts memory per 2 channels
- 16 digital IO channels (Logic Analyzer)

! GOT CURIOUS? ASK FOR YOUR FREE PERSONAL TEST DEVICE.

RIGOL Technologies EU GmbH | Phone +49 89 8841895-0 | info-europe@rigol.com | www.rigol.eu/oscilloscopes | UK distribution partners: www.rigol.eu/sales

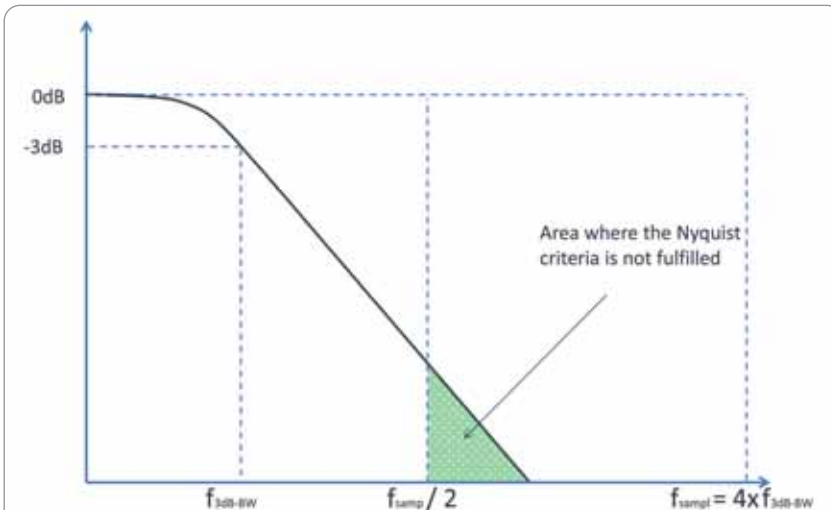


Figure 3: Shifting the sampling rate helps dramatically decrease the area where aliasing will occur



Figure 4: Display of a sine wave with random noise in Normal mode



Figure 5: Display of the Figure 4 signal in High Resolution mode

would be square shaped: flat from zero to the needed bandwidth and a falling edge with an infinitely high slope. Since the real world is far removed from the ideal, we have to live with less sharp filter slopes.

Developing filters with very sharp slopes will quickly lead to very complex filter designs, with high possibility that the filter will become unstable and suffer from self-oscillation problems.

The important parameters for the correct, so-called 'anti-aliasing filter', are a pass area with less ripple, a constant group delay over the whole frequency range and low overshoot at the cutoff frequency. These will allow the input signal to pass as undistorted as possible, keep its integrity high and not affect its accurate analysis at the input of the oscilloscope. However, to realize these requirements, including the very sharp filter slope, is less likely, or it may end up in the most complex of designs.

The second possible solution is using a fairly simple filter with a slow falling edge (typically 6dB/octave), without big overshoots. However, here an ADC with a much higher sample rate is required.

Figure 3 shows that, due to the shift of the sampling rate, the area where aliasing will occur has decreased dramatically. Also, the filter attenuation is now high enough to diminish the amplitude of the remaining 'aliased' frequencies to a negligible level.

The input stage of the oscilloscope, therefore, does not need a complex filter with a sharp falling edge. So, a rule of thumb for the ideal ratio between bandwidth and sample rate applies: *The sample rate should be at least 4-5 times higher than the bandwidth of the scope.*

Rigol oscilloscopes are designed to follow this rule and very often offer a 10-times-higher sampling rate than the defined bandwidth of the scope. To prove this let's have a look at the DS2000 series oscilloscope.

DS2000 Series Oscilloscope

The DS2202 is a 200MHz/2-channels/2GSps model. At worst, its sampling rate is 1GS/s per channel for a 200MHz signal, which means there is still five times oversampling available. At best, we have 2GS/s for a 200MHz signal available, which means that signals up to 1GHz passing through the input stage will not suffer from aliasing. The other models in the DS2000 series with lower frequency (70MHz, 100MHz) have, in best case, more than 20 times oversampling.

An additional positive side-effect of the high sampling rate is that all extra points acquired can be used to realize an extra function, which is called High Resolution (High Res) acquisition. This will help increase theoretically the resolution of the ADC, with calculated additional resolution enhancements of up to 4 bits, depending on the oversampling factor. Furthermore, the displayed noise will be reduced, as the neighbouring points are averaged and, as such, a much cleaner curve will be displayed (see Figures 4 and 5). ●



AVAILABLE
NOW

DISPLAY
MADE EASY

EVE EMBEDDED VIDEO ENGINE

A REVOLUTIONARY
SOLUTION ENABLING
HI-QUALITY, HUMAN
MACHINE INTERFACES
AT A LOWER COST



DEVELOPMENT
SYSTEMS FROM

\$35



DISPLAY AUDIO TOUCH



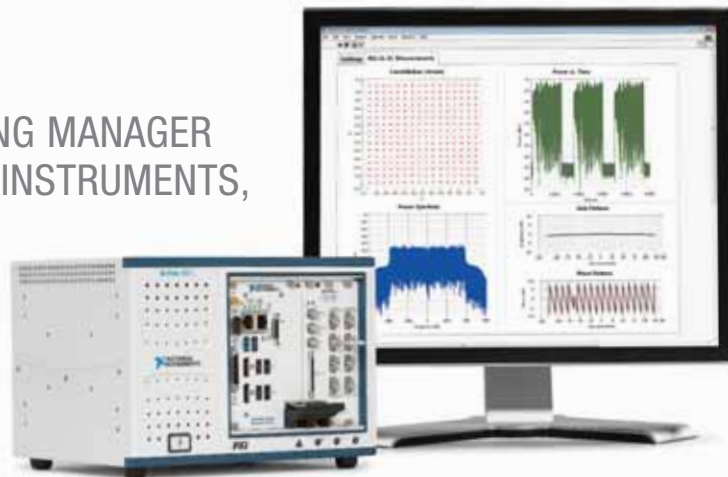
WATCH EVE
DEMOS ONLINE



FTDICHIP.COM

TIPS FOR MAKING THAT TOUGH THIRD-ORDER INTERCEPT MEASUREMENT

NIKHIL AYER, PRODUCT MARKETING MANAGER FOR TEST SYSTEMS AT NATIONAL INSTRUMENTS, HELPS DESIGNERS ENSURE MEASUREMENT ACCURACY IN THEIR NEXT HIGH-LINEARITY THIRD-ORDER INTERCEPT (IP3) MEASUREMENTS



Engineers frequently perform third-order intercept (IP3) measurements to better understand the linearity of a device under test. IP3 measurements at high-power levels (+40dBm and higher) are often some of the most difficult measurements to make. One reason for this is that to obtain an accurate measurement, the third-order distortion products of both the source and signal analyzer must be smaller (ideally 20dB less) than the distortion products introduced by the device under test (DUT). Given the difficulty of making high-linearity IP3 measurements, the following techniques can help you ensure measurement accuracy.

When making an IP3 measurement, you can start by producing a highly linear two-tone source. Although a vector signal generator in “multitone mode” is one way to produce a two-tone signal, this solution usually does not have sufficient distortion performance for the most demanding IP3 measurements.

Instead, the best method to produce a clean two-tone signal is

to use two signal generators through a combiner. Here, source isolation is the key to a successful IP3 measurement, since RF energy from one source can leak into the other.

The Importance of Source Isolation

Several methods can be used to combine signals from two sources to produce isolation sufficient for a difficult IP3 measurement. One obvious requirement is to choose a combiner with the best port-to-port isolation. In general, purely resistive splitter/combiners enable only 6dB to 12dB of isolation. By contrast, Wilkinson power combiners often produce the best isolation, usually offering 20dB or better.

In addition to appropriately choosing the power combiner, you can further isolate the two signal sources. One of the simplest approaches is an isolator or directional coupler. Couplers and isolators frequently provide 30dB of directivity or greater. Along with a Wilkinson power combiner, a configuration using directional couplers at both sources yields better than 50dB of isolation between sources.

With the two-tone source signal appropriately configured, the next step is to analyze the intermodulation products of the stimulus signal to verify that the intermodulation distortion (IMD) is sufficiently low. When using an RF signal analyzer, squeezing out the last few decibels of dynamic range requires a basic understanding of the receiver’s front end. With most RF signal analyzers, you can adjust several settings to improve the IP3 floor of the instrument.

One such setting is RF attenuation, which you can usually control manually or by adjusting the instrument’s reference level. This

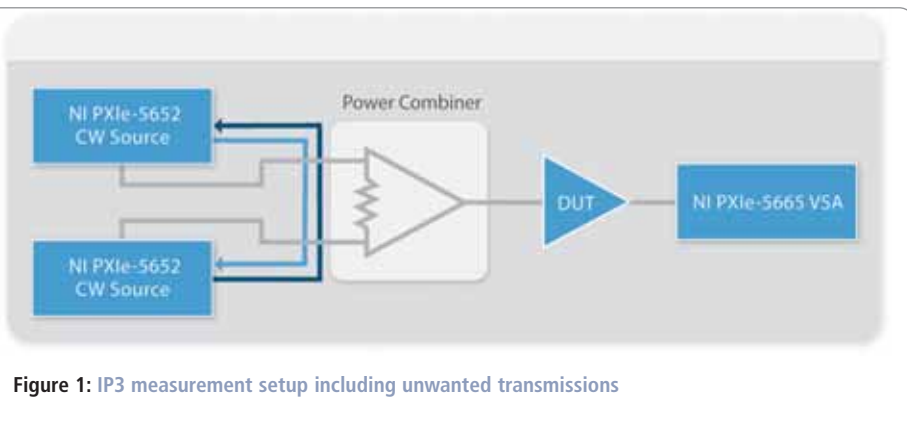


Figure 1: IP3 measurement setup including unwanted transmissions

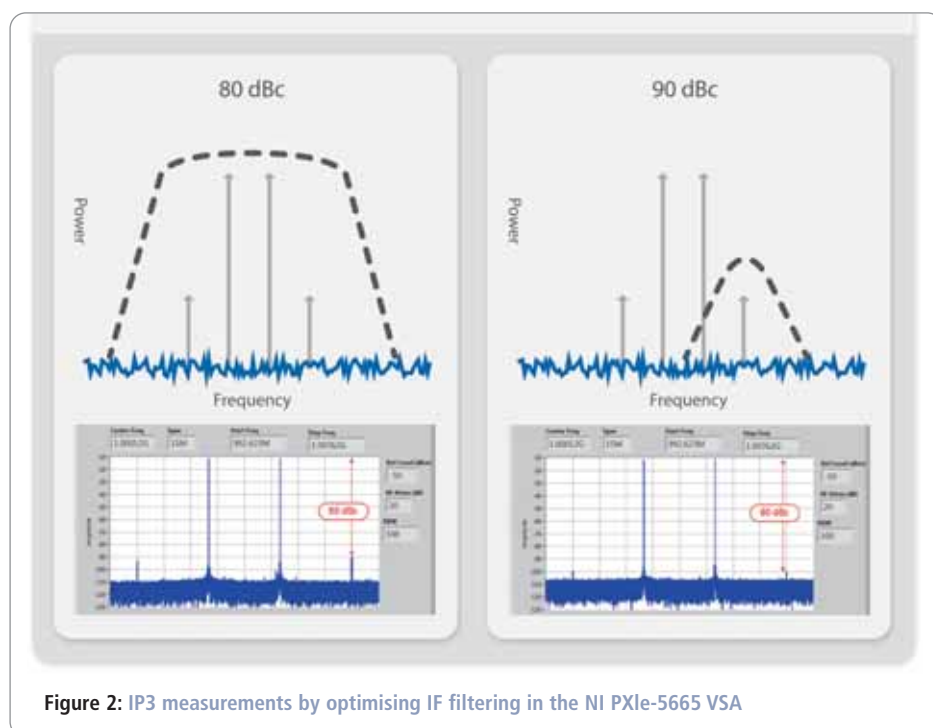


Figure 2: IP3 measurements by optimising IF filtering in the NI PXIe-5665 VSA

setting uses an RF step attenuator to control the input level the rest of the receiver chain sees, which is called the mixer level.

An easy way to determine if your RF signal analyzer is contributing to IP3 or third-order intercept measurement error is to slowly increase the front-end attenuation while observing third-order intermodulation products.

As you increase attenuation, you're effectively reducing the signal level at the first mixer and thereby reducing distortion introduced in the instrument. If the intermodulation products decrease in power as attenuation increases, you can quickly deduce that your instrument is contributing to the measurement error. However, if third-order products remain constant with an increase in attenuation, you can be certain that these intermodulation products are coming from your DUT.

Another Technique

A second technique for reducing distortion inherent to an RF signal analyzer is IF signal conditioning. To prevent clipping, you typically configure the gain of the analyzer to use an IF power level for it is that slightly less than the full scale of the analogue-to-digital converter (ADC).

You can improve the noise floor of the instrument by setting a narrow IF bandwidth and increasing the IF power level. To accomplish this, you have to space the distortion tones so they exceed the bandwidth of the analyzer's IF filter. The figure above depicts an example of this implementation. By filtering out the two-tone stimulus, you reduce the distortion products internally generated

to generate a clean two-tone source with sufficient isolation and configure the RF signal analyzer appropriately. As devices continue to advance, you may have more difficulty measuring IP3 and may need to invest in best-in-class instruments to measure this sensitive but important specification. ●

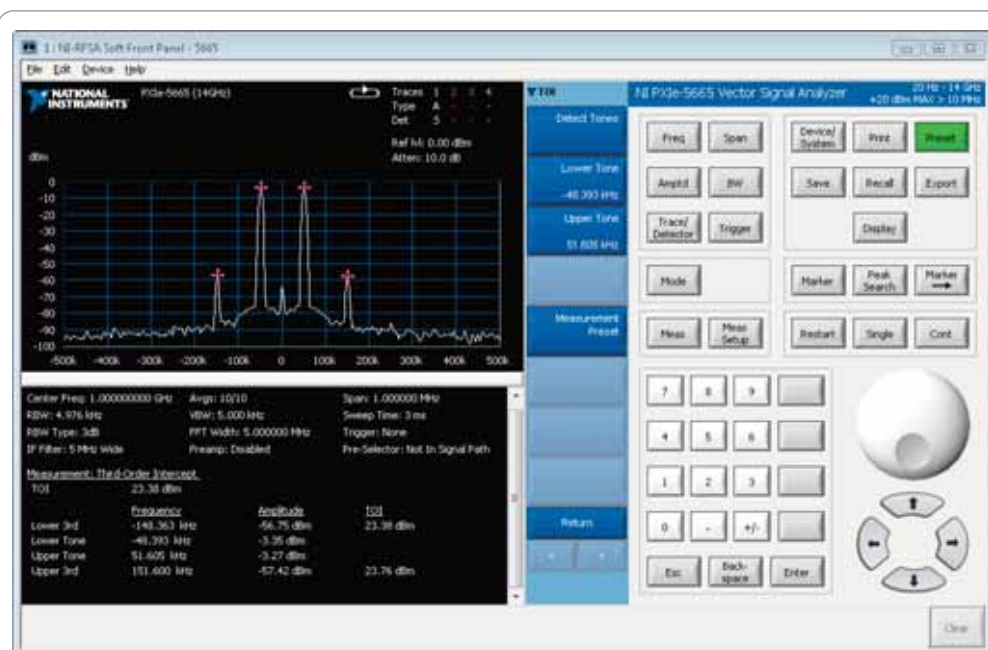


Figure 3: As devices continue to advance, a best-in-class instrument might be needed to successfully measure IP3

FURTHER INFORMATION

To learn more about NI test products and solutions to help meet the toughest measurement challenges, visit ni.com/rf

A ROBUST HIGH-VOLTAGE SQUARE-WAVE SIGNAL GENERATOR WITH ADJUSTABLE FREQUENCY

BY SHAOPENG GUAN, FUGUO DONG, CHANGXIN NAI AND WENYAN SUN
FROM THE SHANDONG INSTITUTE OF BUSINESS AND TECHNOLOGY IN CHINA

In this article, we are describing our design of a robust high-voltage square-wave signal source with adjustable frequency. The design utilizes four IGBTs (Insulated Gate Bipolar Translators) to form a full-bridge circuit powered by a high-voltage DC power supply. A PLC (Programmable Logic Controller) module that produces PWM (Pulse Width Modulation) signals controls the IGBT full-bridge circuit through an IGBT driver board. Then, the high-voltage square-wave

signals of variable frequency are produced as the frequency of the PWM signal changes. The whole circuit is illustrated in Figure 1.

The output of the high-voltage DC power supply is controlled by a low-voltage signal between 0 and 5V provided by the PLC module. The maximum output values are 1000V and 1A, respectively. Four IGBTs in the full-bridge circuit are powered by the high-voltage DC power supply. IGBT1 with IGBT4 and IGBT2 with IGBT3 are switched on in turn under control of the PWM signal, generating the high-voltage square wave signals. The PLC module and the PC are connected through the RS-485 port. Parameters of the high-voltage square-wave signal are controlled by the PLC module.

PLC Module

In the system, the PLC module needs two analogue outputs for control and two analogue inputs for querying the voltage and current outputs of the high-voltage DC power supply, one PWM signal output to control the switching of the IGBT full-bridge circuit and one PTO (Pulse Train Output) signal to display the communication status of the system. We used the Siemens S7-224XP PLC and the Siemens EM232 analogue output module to achieve the above design requirements. PLC I/O (Input/Output) points are shown in Table 1. The I/O connections are shown in Figure 2.

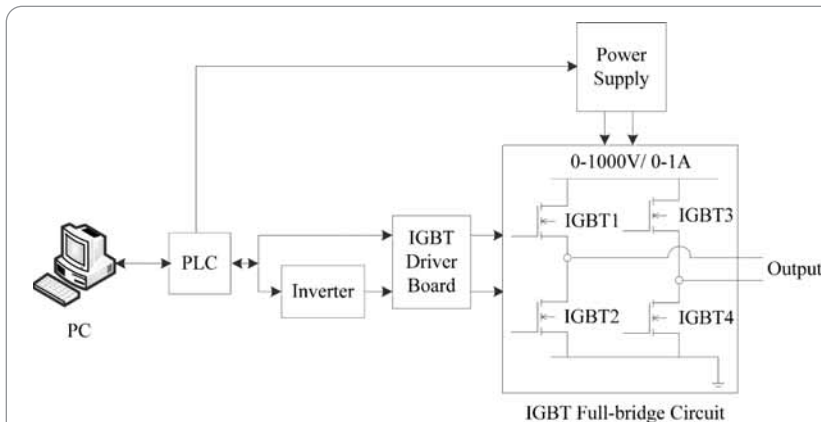


Figure 1: Circuit diagram of the high-voltage square-wave signal generator

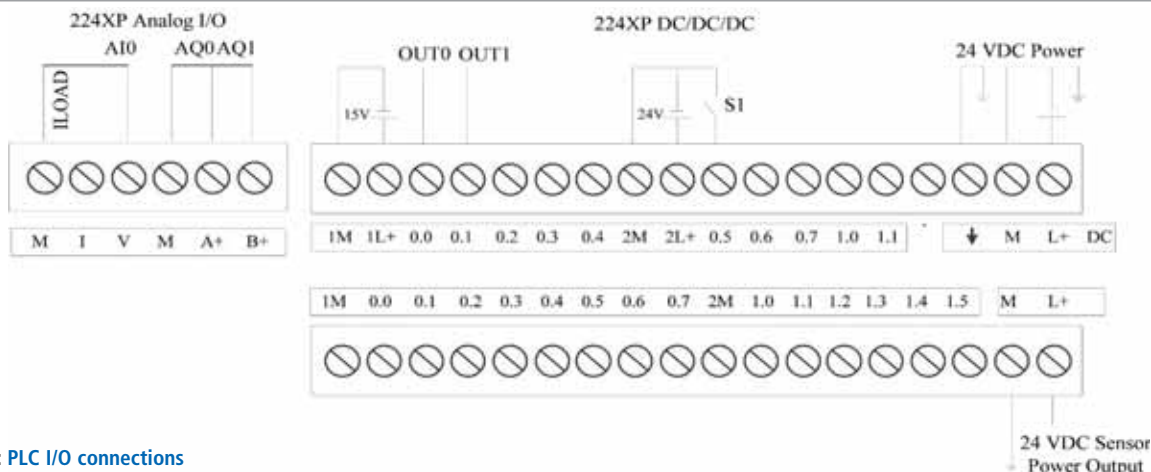


Figure 2: PLC I/O connections

Address allocation	Code	Function
AQW0	AQ0	Voltage output control
AQW2	AQ1	Current output control
AIW0	AI0	Voltage output query
AIW2	AI1	Current output query
Q0.0	OUT0	PWM output
Q0.1	OUT1	PTO output

Table 1: Allocation of PLC I/O points

The Siemens S7-224XP PLC is equipped with a standard RS485 serial communication port. The PC can be connected to the PLC via a RS232-RS485 converter. When the PLC communication port is set to the free-port mode, communications between the PC and the PLC will be fully controlled by the user's program. The so-called free-port mode is the communication that is based on the physical RS485 port but controlled by the user's program. Some communication protocols are also defined by the user.

The control word to set the RS485 port in the free-port mode is stored in special register SMB30 or SMB130. The format of the control word is shown in Table 2.

The Siemens S7-224XP PLC uses standard STEP 7 packages for programming. The sending command is XMT with a format of XMT TABLE PORT. In the command, the TABLE field is a buffer of

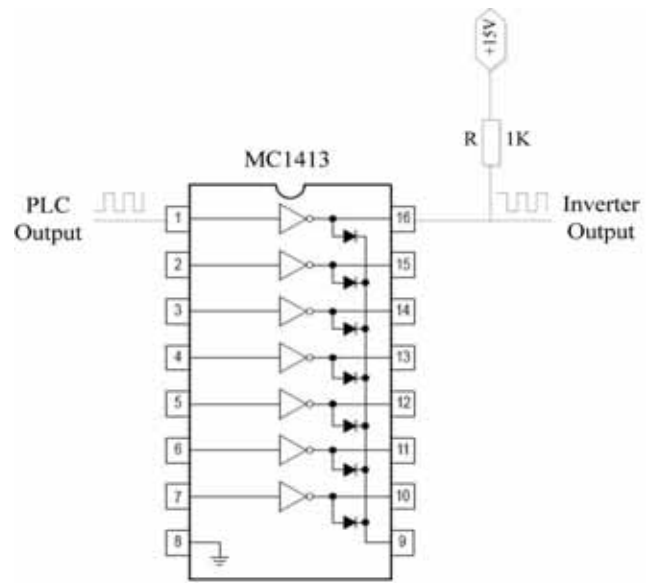



Figure 3: Inverter circuit

the sending information with a data structure of N+DATA+FCS. N is the number of bytes of the data; it must be 0 under the free-port communication mode. FCS is the checksum used for checking the data. PORT is the port used to send data.


The receiving command is RCV with a format of RCV TABLE



UK designed,
UK made,
with pride.

Tel. 01298 70012
www.peakelec.co.uk
sales@peakelec.co.uk

Atlas House, 2 Kiln Lane
 Harpur Hill Business Park
 Buxton, Derbyshire
 SK17 9JL, UK

Follow us on twitter
 for tips, tricks and
 news.
 @peakatlas

For insured UK delivery:
 Please add £3.00 inc VAT
 to the whole order.
 Check online or
 give us a call for
 overseas pricing.


PEAK®
 electronic design ltd

UTP05 Network Cable Analyser

RJ45 based Cat5/5e/6 Support

Identify and Fault-Find your computer cabling

- Automatically identify and test patch cables, crossover cables, token ring, mixed voice/data and many other configurations.
- Identify all types of fault including breaks, shorts and swaps.
- Analyses all 8 lines in your cabling.
- Works with 4 line cables too.
- Padded case with spaces for instrument and all accessories.
- Includes alkaline battery (and spare).
- Very comprehensive user guide including colour cabling diagrams.
- Complete with 2 remote compact terminators.
- Includes 2 mini patch cables for socket testing.
- User friendly display with full descriptions.
- UK designed and made.




Items included **£77.95**
£64.96+VAT

DCA75 DCA Pro

The all new "A very capable analyser"


Exciting new generation of semiconductor identifier and analyser. The **DCA Pro** features a new graphics display showing you detailed component schematics. Built-in USB offers amazing PC based features too such as curve tracing and detailed analysis in Excel. PC software supplied on a USB Flash Drive. Includes Alkaline AAA battery and comprehensive user guide.



Now Shipping
£115.95
 £96.62+VAT

LCR40

The Atlas LCR (Model LCR40) is now supplied with our new premium quality 2mm plugs and sockets to allow for greater testing flexibility. Includes 2mm compatible hook probes as standard, other types available as an option.



£89.95
£74.96+VAT

Automatically test inductors (from 1uH to 10H), capacitors (1pF to 10,000uF) and resistors (1Ω to 2MΩ). Auto-range and auto component selection.

Automatic test frequency from DC, 1kHz, 15Hz and 200kHz. Basic accuracy of 1.5%.

Battery and user guide included.

It's only possible to show summary specifications here. Please ask if you'd like detailed data. Further information is also available on our website. Product price refunded if you're not happy.

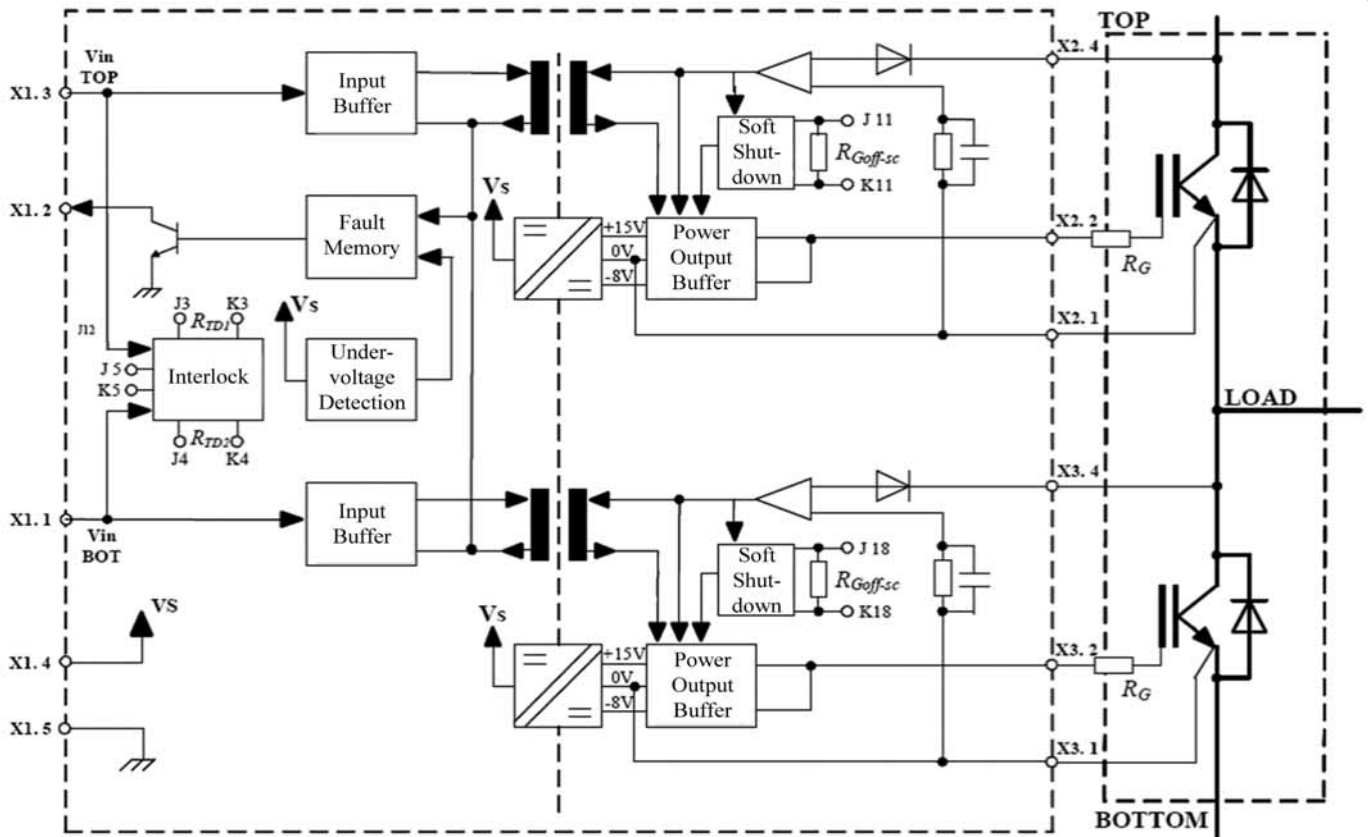


Figure 4: The IGBT driver board

PORT. There are two types of information sent by the PC: commands and common data.

Generating a Square Wave Signal

PTO and PWM signals are generated in high speed outputs Qo.0 and Qo.1 under the command of a PLS (pulse) sent by the PLC.

The PTO signal is a square wave of 50% duty cycles; users can control its duty cycle and number of pulses. The PWM signal is a continuous square wave with variable duty cycles. Its duty cycle and pulse width can be changed by the user. The PTO signal indicates the communication status of the system by making the LED flash.

The PWM signal is used to drive the switching of IGBTs to generate the high-voltage square-wave signal. The PWM signal is divided into two branches: one is directly connected to the IGBT driver board; the other is inverted and then connected to the IGBT driver board. The inverter circuit is the Darlington transistor array MC1413, which can handle high voltage and large current. The inverter can be directly connected to the output of the PLC and produce an inverted signal. Two signals of opposite phase control the switching of four IGBTs in the full-bridge circuit signal through the IGBT driver board. The high-voltage square-wave signal is generated when IGBT1 with IGBT4 and IGBT2 with IGBT3 are turned on in turn. The inverter circuit is shown in Figure 3.

The IGBT driver board is used to guarantee the proper operation of the IGBT module and at the same time protect the circuit. The circuit diagram of the IGBT driver board is illustrated in Figure 4. The IGBTs are Fairchild FGL60N170D with a breakdown voltage of 1700V between collector and emitter. ●

PP (Check type)	00		No check	
	01		Even check	
	10		No check	
	11		Odd check	
D (Bits per character)	0		8 bits	
	1		7 bits	
BBB (baud rate)	000	38400 bps	100	2400 bps
	001	19200 bps	101	1200 bps
	010	9600 bps	110	600 bps
	011	4800 bps	111	300 bps
MM (Protocol type)	00		PPI/ Slave mode (default)	
	01		Free-port mode	
	10		PPI/ Master mode	
	11		Reserved field	

Table 2: Control word format of PLC communication

A complete system with intelligence!



Make no compromises with system quality –
connector and assembly from one source.



As a specialist for custom-specific connection systems, we have the
system solution with added value for even your most extreme requirements –

ODU-UK Ltd
Phone: 01509/26 64 33
sales@odu-uk.co.uk

SPECIAL OFFERS
for full sales list
check our website

www.stewart-of-reading.co.uk

Check out our website, 1,000's of items in stock.

Used Equipment – **GUARANTEED**
All items supplied as tested in our Lab
Prices plus Carriage and VAT

AGILENT	E4407B	Spectrum Analyser – 100HZ-26.5GHZ	£6,500	MARCONI	2955	Radio Comms Test Set	£595
AGILENT	E4402B	Spectrum Analyser – 100HZ-3GHZ	£3,500	MARCONI	2955A	Radio Comms Test Set	£725
HP	3325A	Synthesised Function Generator	£250	MARCONI	2955B	Radio Comms Test Set	£850
HP	3561A	Dynamic Signal Analyser	£800	MARCONI	6200	Microwave Test Set	£2,600
HP	3581A	Wave Analyser – 15HZ-50KHZ	£250	MARCONI	6200A	Microwave Test Set – 10MHZ-20GHZ	£3,000
HP	3585A	Spectrum Analyser – 20HZ-40MHZ	£995	MARCONI	6200B	Microwave Test Set	£3,500
HP	53131A	Universal Counter – 3GHZ	£600	IFR	6204B	Microwave Test Set – 40GHZ	£12,500
HP	5361B	Pulse/Microwave Counter – 26.5GHZ	£1,500	MARCONI	6210	Reflection Analyser for 6200Test Sets	£1,500
HP	54502A	Digitising Scope 2ch – 400MHZ 400MS/S	£295	MARCONI	6960B with 6910	Power Meter	£295
HP	54600B	Oscilloscope – 100MHZ 20MS/S from	£195	MARCONI	TF2167	RF Amplifier – 50KHZ-80MHZ 10W	£125
HP	54615B	Oscilloscope 2ch – 500MHZ 1GS/S	£800	TEKTRONIX	TD53012	Oscilloscope – 2ch 100MHZ 1.25GS/S	£1,100
HP	6030A	PSU 0-200V 0-17A – 1000W	£895	TEKTRONIX	TD5540	Oscilloscope – 4ch 500MHZ 1GS/S	£600
HP	6032A	PSU 0-60V 0-50A – 1000W	£750	TEKTRONIX	TD5620B	Oscilloscope – 2+2ch 500MHZ 2.5GHZ	£600
HP	6622A	PSU 0-20V 4A twice or 0-50v2a twice	£350	TEKTRONIX	TD5684A	Oscilloscope – 4ch 1GHZ 5GS/S	£2,000
HP	6624A	PSU 4 Outputs	£350	TEKTRONIX	2430A	Oscilloscope Dual Trace – 150MHZ 100MS/S	£350
HP	6632B	PSU 0-20V 0-5A	£195	TEKTRONIX	2465B	Oscilloscope – 4ch 400MHZ	£600
HP	6644A	PSU 0-60V 3.5A	£400	TEKTRONIX	TFP2A	Optical TDR	£350
HP	6654A	PSU 0-60V 0-9A	£500	R&S	APN62	Synthesised Function Generator – 1HZ-260KHZ	£225
HP	8341A	Synthesised Sweep Generator – 10MHZ-20GHZ	£2,000	R&S	DPSP	RF Step Attenuator – 139db	£400
HP	8350B with 83592a	Generator – 10MHZ-20GHZ	£600	R&S	SME	Signal Generator – 5KHZ-1.5GHZ	£500
HP	83731A	Synthesised Signal Generator – 1-20GHZ	£2,500	R&S	SMK	Sweep Signal Generator – 10MHZ-140MHZ	£175
HP	8484A	Power Sensor – 0.01-18GHZ 3nW-10uW	£125	R&S	SMR40	Signal Generator – 10MHZ-40GHZ with options	£13,000
HP	8560A	Spectrum Analyser synthesised – 50HZ -2.9GHZ	£2,100	R&S	SMT06	Signal Generator – 5KHZ-6GHZ	£4,000
HP	8560E	Spectrum Analyser synthesised – 30HZ-2.9GHZ	£2,500	R&S	SW0B5	Polyscope – 0.1-1300MHZ	£250
HP	8563A	Spectrum Analyser synthesised – 9KHZ-22GHZ	£2,995	CIRRUSS	CL254	Sound Level Meter with Calibrator	£60
HP	8566A	Spectrum Analyser – 100HZ-22GHZ	£1,600	FARNELL	AP60/50	PSU 0-60V 0-50A 1KW Switch Mode	£250
HP	8662A	RF Generator – 10KHZ-1280MHZ	£1,000	FARNELL	H60/50	PSU 0-60V 0-50A	£500
HP	8672A	Signal Generator – 2-18GHZ	£500	FARNELL	B30/10	PSU 30V 10A Variable No meters	£45
HP	8673B	Synthesised Signal Generator – 2-26GHZ	£1,000	FARNELL	B30/20	PSU 30V 20A Variable No meters	£75
HP	8970B	Noise Figure Meter	£995	FARNELL	XA35/2T	PSU 0-35V 0-2A twice Digital	£75
HP	33120A	Function Generator – 100 microHZ-15MHZ	£395	FARNELL	LF1	Sine/sq Oscillator – 10HZ-1MHZ	£45
MARCONI	2022E	Synthesised AM/FM Sig Generator – 10KHZ-1.01GHZ	£395	STEWART OF READING 17A King Street, Mortimer, Near Reading, RG7 3RS Telephone: 0118 933 1111 • Fax: 0118 933 2375 9am – 5pm, Monday – Friday Please check availability before ordering or CALLING IN			
MARCONI	2024	Synthesised Signal Generator – 9KHZ-2.4GHZ from	£800				
MARCONI	2030	Synthesised Signal Generator – 10KHZ-1.35GHZ	£950				
MARCONI	2305	Modulation Meter	£250				
MARCONI	2440	Counter 20GHZ	£395				
MARCONI	2945	Comms Test Set various options	£3,000				

DESIGN OF A MICROCONTROLLER-BASED BODY HEIGHT MEASURING DEVICE

PROFESSOR **DOGAN IBRAHIM** OF THE NEAR EAST UNIVERSITY IN CYPRUS DESCRIBES THE DESIGN OF A MICROCONTROLLER-BASED BODY HEIGHT MEASURING DEVICE USING ULTRASONIC TECHNIQUES

M

aintaining a healthy weight is important for protection against several disabilities and obesity-related illnesses. Equally, reaching the correct height for a child's age is important, so a problem can be detected at an early stage and appropriate treatment undertaken in time.

Several factors may affect the height of a growing child, such as medications used, kidney failure, intestinal disorders that may affect the absorption of nutrients, cystic fibrosis, childhood diabetes and hereditary genetic factors.

Some known conditions that may affect a person's height are:

- **Aging and osteoporosis:** It is known that people tend to lose height as a result of aging and osteoporosis. On average women lose about two inches over their lifetimes, while men lose about an inch.
- **Reduced/increased growth hormone:** Children with reduced growth hormone tend to have lower heights. On the other hand, excessive growth hormone during puberty may lead to an excessive height, as in gigantism.
- **Hypothyroidism:** A deficiency of thyroid hormone during childhood may lead to short height.
- **Hypogonadism:** This is another hormone-related condition caused by the reduction of sex hormones that may affect the height, especially during puberty.
- **Medication:** It is known that certain types of medicines given during childhood and taken for prolonged periods may disturb the growth of the child. For example, some anti-inflammatory medications prescribed for asthma, ulcerative colitis and bone disorders may affect growth.
- **Childhood bone disorders:** Some children develop joint inflammation and bone disorders at very early stages of their growth. Such conditions may affect the bone development and, consequently, lead to reduced height.
- **Poor nutrition:** If children do not follow a balanced diet or if intake of food is inadequate for their growth, body height may also be affected.
- **Exercise:** Physical activities, such as sports or stretch exercises can also increase a person's height.
- **Heredity:** This plays a major role in deciding the physical attributes of a person, such as physical appearance, physical

features, complexion, height and weight. It is well-known that body height can be hereditary and may also depend upon the race of the person.

It is important that the height and weight of growing children be measured at regular intervals and records kept so any growth problems can be recognised at an early stage. Usually height-weight charts based on body mass index are used to assess the weight and height of a person. Depending upon these charts a person may fall into one of four categories: underweight, normal weight, overweight, or obese.

Measuring Height

The body height of a person can be measured using a simple tape measure, or more professionally by using a device called a stadiometer. Stadiometers can be mechanical or electronic. As shown in Figure 1, a mechanical stadiometer simply consists of a long pole with heights marked on it either in mm or cm, usually mounted on a wall. An adjustable spacer is moved so it touches the top of the head of a person. The height is then read on the pole at the spacer's pointer (see Figure 2). The measuring range of a mechanical stadiometer is usually around 20-205cm.

Although relatively cheap, mechanical stadiometers are not very accurate; the spacer may become loose with aging, and measurement takes time, especially when measurements are required in a school or club. As an example, consider the case of measuring the height of 500 children in a school using a mechanical stadiometer. If we assume that each measurement



Figure 1: Mechanical stadiometer

takes about two minutes, it will require several days' full-time work to measure the height of all the children.

Electronic (also called digital) stadiometers are similar to mechanical ones in shape and look (see Figure 3), but instead of having scales on the pole, a fixed transmitter-receiver sensor module is mounted on top of the assembly and there is no moving spacer. The person to be measured stands under the sensor module. The distance from the sensor to the top of person's head is measured by an electronic system which is part of the stadiometer. The height of the person is calculated and displayed on an LCD by knowing the distance of the sensor from the floor. Although most electronic stadiometers use ultrasonic sensors, some can be infrared.

There are various forms of electronic stadiometers available on the market: some operate wirelessly, where the measured height is transmitted to a PC using wireless communication, for example Bluetooth; some have printers attached to print the height; some are connected to a PC using cables (e.g. USB); some have auto-zero adjustment facilities; and so on.

Electronic stadiometers are very accurate and the actual measurement takes only a few seconds. In addition, on some models, the measured data can be printed or sent to a PC automatically if desired.

In this article we present the design of an electronic stadiometer using a microcontroller and a pair of ultrasonic sensors, for transmitting and receiving. For simplicity, the measured height is displayed on an LCD.

Design of the Electronic Stadiometer

A diagram of a design of an electronic stadiometer is shown in Figure 4. A pair of ultrasonic sensors, one configured as a transmitter and the other as a receiver, is mounted on a 2m high pole. The sensors are connected to the digital I/O pins of a high-end PIC18 type microcontroller. In addition, a 2x16 character text-based LCD is connected to output ports of the microcontroller.



Figure 3: Typical electronic stadiometer



Figure 2: Reading the height on a stadiometer

Operation of the stadiometer is very simple: During normal operation the microcontroller sends a pulse to the TX sensor and waits to receive the echo signal at the RX sensor. By calculating the elapsed time and knowing the speed of sound in air, the microcontroller calculates the distance from the sensor assembly to the top of the person's head. The person's height is then determined by subtracting this distance from 2m, and then displayed on the LCD.

The Hardware

The hardware makes use of the Ready For PIC microcontroller development board (see Figure 5), which is equipped with a PIC18F45K22 high-end microcontroller chip, 8MHz crystal, FTDI chip, power regulator circuit, I/O port connectors and a breadboard area.

The board is connected to a PC via the USB port, and the developed code is loaded onto the program memory of the microcontroller via this port. In addition, a debugger interface

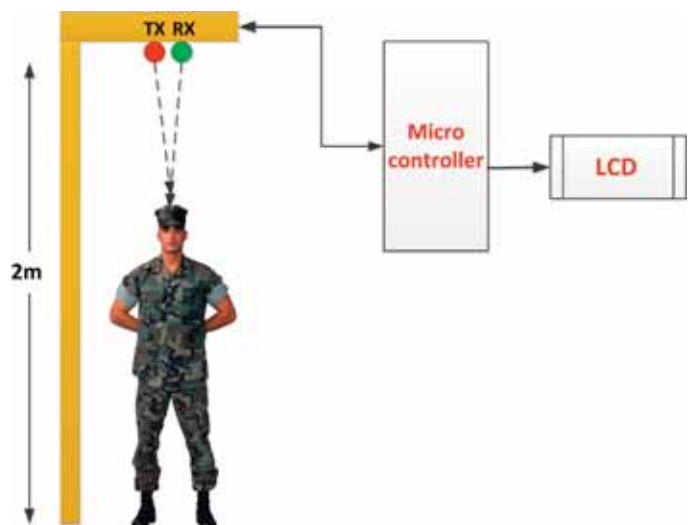


Figure 4: Diagram of an electronic stadiometer

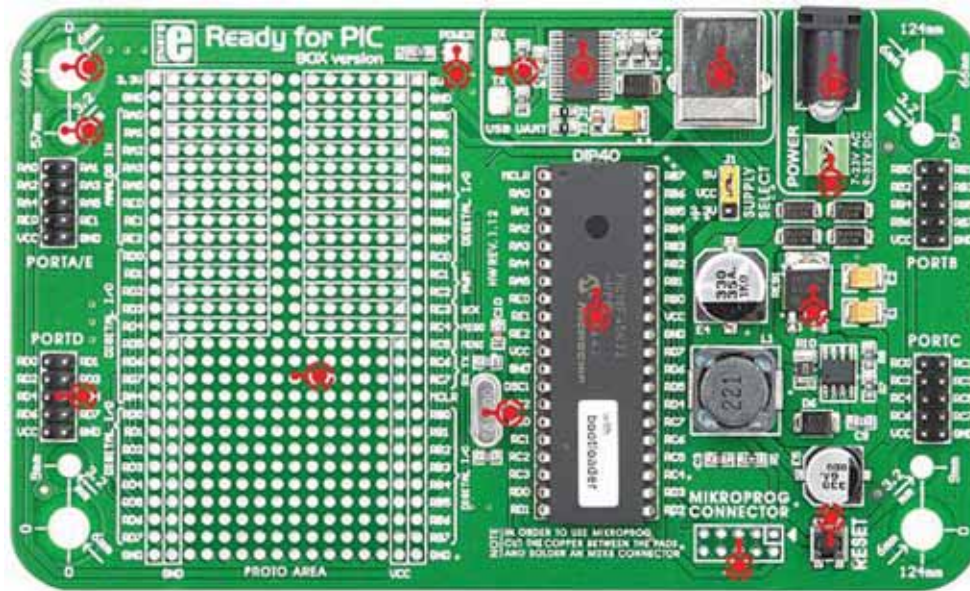


Figure 5: 'Ready For PIC' development board

(Microprog debugger) is provided for fast debugging during program development.

Figure 6 shows the circuit diagram of the stadiometer. The ultrasonic sensor module is connected to port pin RD0 of the microcontroller, which is configured in software both as an input and output pin. PORT B is connected to the 2x16 character LCD.

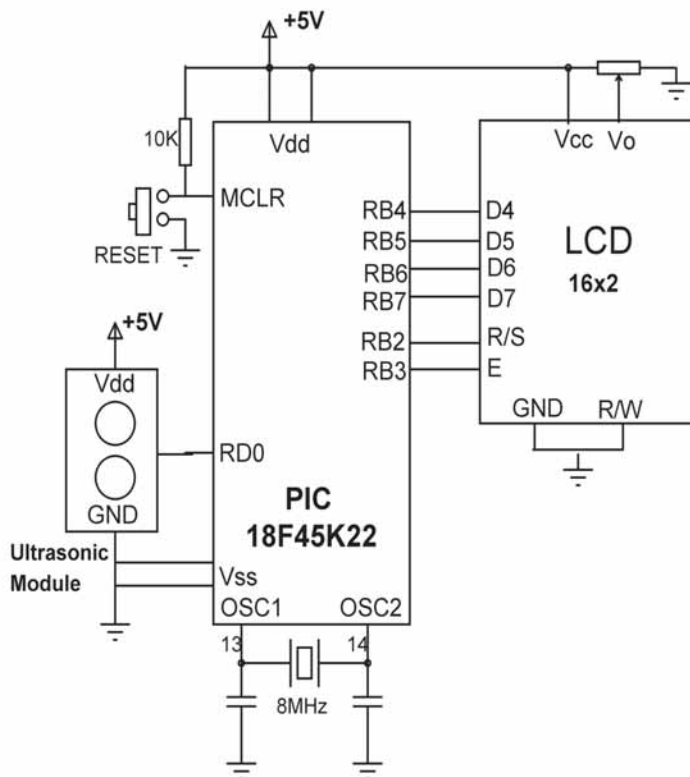


Figure 6: Circuit diagram of the stadiometer

The Ultrasonic Module

The ultrasonic module used in the design is called “PING”, manufactured by Parallax. This module (see Figure 7) consists of two ultrasonic transducers mounted next to each other and used as a pair in distance measurement applications, one used as transmitter and the other as receiver. The module has only three pins: power, ground and signal I/O. The range of the module is 2cm to 3m when used in distance measurements, with an accuracy better than 0.5cm.

The Software

The software has been developed using the highly popular mikroC Pro for PIC compiler. A code-size-limited

demo version of the compiler is available from the developers. The operation of the software is straight-forward and is explained in Code 1, with the full program listing given in Code 2.

At start-up, the LCD interface and the I/O ports are configured and the LCD is initialised by calling to library function LCD_Init(). Then timer 0 of the microcontroller is configured to count in 16-bit mode with a counting rate of 1μs. The rest of the code executes in an endless loop. Here, initially the timer is cleared to zero, a pulse sequence is sent to the ultrasonic sensor (TX) and the timer starts the count. This pulse hits the target (top of the person's head) and returns as an echo. As soon as the echo signal is received the timer is stopped and the elapsed time is calculated in microseconds. The distance to the target is then calculated as follows:

Let T_m be the elapsed time stored in the timer in microseconds. The time T_t for the signal to reach the target is then given by $T_t = T_m/2$. Assuming that the speed of sound in air is 340m/s (this is true at 15°C), this corresponds to 0.034cm/μs. Thus, the distance h to the target is given by:

$$h = 0.034 \times T_t$$

If the distance between the sensors and the ground level is 2m, then the height H of the person in cm is simply found as:

$$H = 200 - h$$

The above process is repeated continuously with a one-second delay between measurements.

Tests

Tests carried out with this design of stadiometer show an accuracy of better than 0.5cm. The project can be improved further as suggested below:

- Auto-zero facility can be added such that the stadiometer can measure the distance to ground on start-up and then initialise itself automatically.
- The stadiometer can be connected to a PC either using wires, or for example using wireless communication such as Bluetooth. The measured height can then be sent and stored automatically in a database on the PC together with the personal details of the person.

- The accuracy of the measurement can be increased by taking into account the effect of temperature on the speed of sound, but if auto-zero is added then temperature effects will automatically be taken into consideration. ●



Figure 7: The ultrasonic module

```
BEGIN
  Configure I/O ports
  Configure the timer
  DO FOREVER
    Clear timer
    Send a pulse sequence to TX
    Start timer
    Wait for echo
    Stop timer
    Calculate time to the target
    Calculate distance to target
    Calculate and display distance to target
    Wait for one second
  ENDDO
END
```

Code 1: Operation of the software

```
// LCD module connections
sbit LCD_RS at LATB2_bit;
sbit LCD_EN at LATB3_bit;
sbit LCD_D4 at LATB4_bit;
sbit LCD_D5 at LATB5_bit;
sbit LCD_D6 at LATB6_bit;
sbit LCD_D7 at LATB7_bit;
sbit LCD_RS_Direction at TRISB2_bit;
sbit LCD_EN_Direction at TRISB3_bit;
sbit LCD_D4_Direction at TRISB4_bit;
sbit LCD_D5_Direction at TRISB5_bit;
sbit LCD_D6_Direction at TRISB6_bit;
sbit LCD_D7_Direction at TRISB7_bit;
// End of LCD module connections

// Ultrasonic module connection
sbit Ultrasonic at RD0_bit;
sbit Ultrasonic_Direction at TRISD0_bit;

/***** BEGINNING OF MAIN PROGRAM *****/
void main()
{
  unsigned long Tt;
  unsigned char Tl, Th;
  unsigned int h, H;
  char Txt[7];

  ANSELB = 0; // PORT B is digital
  ANSELD = 0; // PORT D is digital
  T0CON = 0x02; // Configure Timer0: 16-bit mode,
1us count
  //
  // Send a pulse, start timer, get echo, stop timer, calculate
distance and display
  //
  for(;;)
  {
    Ultrasonic_Direction = 0; // PORT D bit 0 in output mode

    TMR0H = 0; // Clear high byte of timer
    TMR0L = 0; // Clear low byte of timer
    Ultrasonic = 0;
    Delay_us(3);
    Ultrasonic = 1; // Send a PULSE to Ultrasonic
module
    Delay_us(5);
    Ultrasonic = 0;
    Ultrasonic_Direction = 1; // PORT D bit 0 in input
mode
    while(Ultrasonic == 0); // Wait until echo is received
    T0CON.TMR0ON = 1; // Start timer
    while(Ultrasonic == 1); // Wait until echo ready
    T0CON.TMR0ON = 0; // Stop timer
    Tl = TMR0L; // Read timer low byte
    Th = TMR0H; // Read timer high byte
    Tt = Th*256 + Tl; // Timer as 16 bit value
    //
    // Now find the distance and body height
    //
    Tt = Tt / 2; // Half the time
    Tt = 34 * Tt;
    Tt = Tt / 1000; // Divide by 1000
    h = (unsigned int)Tt;
    H = 200 - h; // Body height
    //
    // Now display the body height
    //
    IntToStr(H, Txt); // Convert to string
    Lcd_Cmd(_LCD_CLEAR); // Clear LCD
    Lcd_Out(1,1, "Height (cm)"); // Display the height
    Lcd_Out(2,1, Txt);
    Delay_Ms(1000); // Delay 1 second
  }
}
```

Code 2: Software listing

A DISTRIBUTED IMAGE COMPRESSION ALGORITHM FOR ENVIRONMENTAL MONITORING APPLICATIONS

AYSEGUL ALAYBEYOGLU FROM THE COMPUTER ENGINEERING DEPARTMENT OF CELAL BAYAR UNIVERSITY IN MANISA, TURKEY, PRESENTS A DISTRIBUTED IMAGE COMPRESSION ALGORITHM FOR ENVIRONMENTAL MONITORING APPLICATIONS IN WIRELESS MULTIMEDIA SENSOR NETWORKS

Wireless multimedia sensor networks are composed of tiny, camera-equipped and energy-limited sensor nodes that are capable of sensing, processing and transmitting image data in a networked environment. Because of the resource constraints of sensors, image data should be compressed and the transmission of such large amount of data distributed among the sensor nodes to balance the computational load.

In this article, we propose a distributed image compression

algorithm for environmental monitoring applications using wireless sensor networks. The proposed system operates in two phases: dynamic cluster construction and distributed image compression. In the first phase, when a camera-equipped sensor node receives a query from the base station, it checks its data, and if the query and this data match, it sends a warning message to its neighbouring node to start the process of constructing the clusters in the direction of the base station.

After the clusters are formed dynamically, the second phase of the system comes into play and the camera-equipped sensor node starts sending visual data to the base station in a distributed manner. Simulation results show that the proposed algorithm performs better than a centralized image-compression approach for system lifetime, energy consumption and image quality parameters.

Wireless Sensor Networks

Energy is one of the most significant constraints in sensor network applications, with many techniques used to decrease energy consumption. One such scheme is called “clustering”, where nodes located closely to each other are grouped into a cluster. This increases collaboration between the nodes, which in turn improves the monitoring capability and overall efficiency by distributing the workload [1].

Clusters can be formed dynamically, when an event starts, or statically, at the time of network deployment. In this study we worked with dynamically-created clusters, where the proposed algorithm adapts to the sink's locations from which the queries are received.

In monitoring applications, a base station might need visual data, which may require a high data-rate. Having only one node process and transmit image data using traditional image compression is not suitable for wireless multimedia sensor networks, especially when there are energy constraints imposed on that network. So, in order to balance the computational overhead of the sensor nodes, we recommend a distributed image compression algorithm based on a discrete wavelet transform.

In most image data, neighbouring pixels are correlated with each other, so a lower number of bits can be used to represent an image, eliminating redundant data.

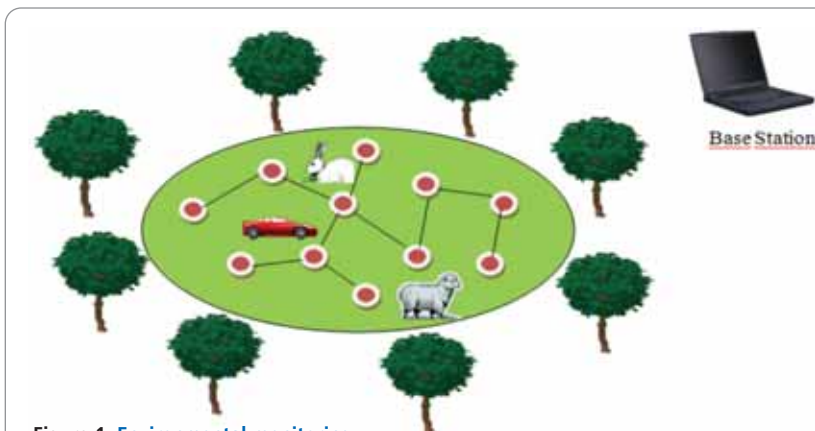


Figure 1: Environmental monitoring

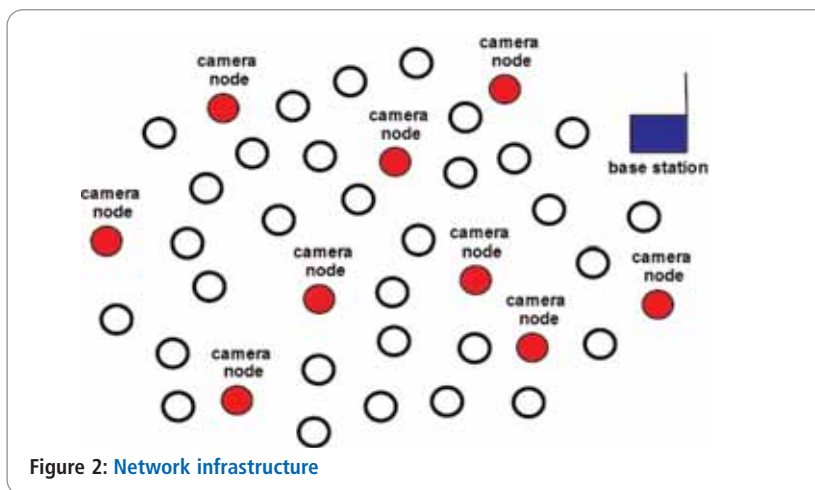


Figure 2: Network infrastructure

Wavelet-based coding is one of the most commonly used schemes for compressing image data. In this scheme, the frequency band of the image data is divided into various sub-bands. Low- and high-pass filters are applied to the rows and columns of the image data to group the content of the image into low and high frequencies. After applying the filters, frequencies of the image data are grouped into four further subbands: LL (low-low), HL (high-low), LH (low-high) and HH (high-high). While low-pass filtering is used for smoothing the image, high pass filtering sharpens it [2].

Environmental Monitoring

Chemical emissions can affect the environment adversely, so many researchers are now focusing on environmental monitoring applications, see Figure 1. Sensors are located in the environment of interest to obtain monitoring data. When the base station needs information about an object moving within that environment, it sends a QUERY message to the nodes. They, in turn, check their data and if there's a match, they send it to the base station using routing protocols.

When a large amount of image data is needed by the base station, the routing is distributed among the other nodes to balance the workload and energy consumption.

The infrastructure of the proposed system can be described as an undirected graph $G(V, E)$ in which the vertices (V) represent the sensor nodes, and the edges (E) represent the communication links between these nodes. Two types of sensor nodes are used in the system: camera-equipped and ordinary nodes. Camera nodes are responsible for capturing visual data and sending it to the base station. Figure 2 shows the system's network infrastructure.

Each node in the network has a unique node ID and its own and neighbours' location information. Each node also has a specified communication range, and if any two nodes are located inside each other's range, they communicate directly.

Dynamic Cluster Construction Phase

When a base station requires information, it flags a QUERY (location of the base station, required information, quality)

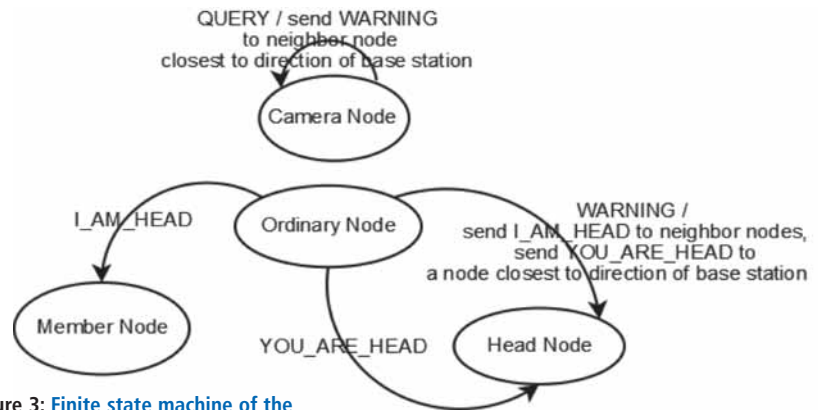


Figure 3: Finite state machine of the dynamic cluster construction

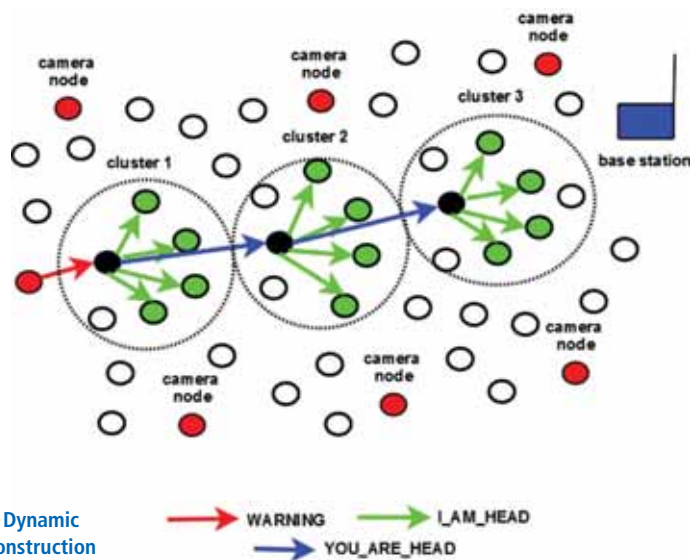


Figure 4: Dynamic cluster construction

message to the network to collect information from the camera sensor nodes. As each camera node receives this QUERY message, it checks its data, and if the query and its data match, it sends a WARNING message to the source of the message.

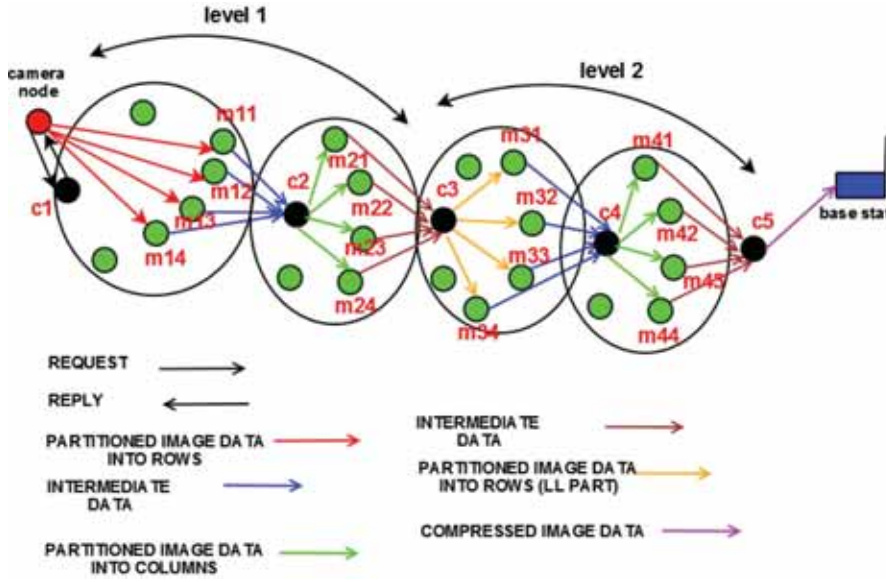
When a node receives a WARNING message, it makes a state transition to the head node and sends an I_AM_HEAD (ID of the next cluster's head node) message to the neighbouring nodes in the direction of the base station, in order to form its cluster. The node that receives this message transitions to a member node and becomes a cluster member of the head node from which it received the message. In order to continue constructing the clusters, the head node sends a YOU_ARE_HEAD (in location of the base station) message to the node which is not a member of its cluster and which is located in the direction of the base station.

When a node receives a YOU_ARE_HEAD message it makes a state transition to head node and forms its cluster by sending an I_AM_HEAD (ID of the next cluster's head node) message to its neighbouring nodes located in the path towards the base station. This cluster construction process continues until the base station is reached. Figure 3 shows the finite state machine of the dynamic cluster construction phase of the system.

In clusters, both ordinary nodes and head nodes are responsible for applying the Distributed Wavelet Transform and sending the compressed data to the base station. Figure 4 shows an example of the dynamic cluster construction phase of the system.

Wavelet-based coding is one of the most commonly used schemes for compressing image data; here, the frequency band of the image data is divided into various sub-bands

Figure 5: Distributed image compression



Distributed Image Compression Phase

The aim of the proposed image compression algorithm is to distribute the computational load of the wavelet transform to the nodes located on the path from the camera node (source) to the base station (destination). This way, a number of nodes are involved in the processing and transfer of data rather than just a single node.

The pseudocode of the proposed distributed image compression algorithm is given in Algorithm 1.

Figure 5 shows an example of distributed image compression from a camera node to the base station. When a camera node receives a QUERY message from the base station that includes the required data, it triggers the cluster construction phase. Following this, the camera node sends a REQUEST message to the closest cluster head (c1) in order to get the IDs of the member nodes in this cluster.

When c1 receives the REQUEST message, it sends a REPLY (ID, c2) message, including the ID of the next cluster head and the IDs of the nodes M1 (m11, m12, m13, m14) in its cluster. The camera node partitions the image data into rows and sends them to M1 (m11, m12, m13, m14) that run a 1D wavelet transform on the received data. The intermediate results are then sent to the head of the next cluster c2, instead of back to c1, as in previous studies [3]-[6]. c2 combines the intermediate results and partitions the image data into columns. It then sends this partitioned data to its member nodes M2 (m21, m22, m23, m24) to complete the single-level wavelet transform. These nodes send the results to the head of the next cluster c3, which selects only the low frequency (LL) part of the image and distributes it to its member nodes M3 (m31, m32, m33, m34) to run a 1D wavelet transform. The intermediate results are then sent to the head of next cluster c4, which combines the intermediate results and partitions the image data into columns. This partitioned data is sent to c4's member nodes M4 (m41, m42, m43, m44) to complete the second-level wavelet transform. This procedure continues until the compressed data is received by the base station, in accordance with the image quality defined in the QUERY message.

The proposed algorithm is different from the studies in literature [3-7], since it works in the forward direction toward the destination. Nodes never send messages to nodes behind them in the chain toward the destination. For example, in Figure 5 the member nodes M2 (m21, m22, m23, m24) send the intermediate results to the head of the next cluster c3 instead of sending them back to c2.

In the proposed distributed image compression algorithm, the image is divided into code blocks which are coded independently. To reduce energy consumption, entropy coding is executed before data exchange occurs.

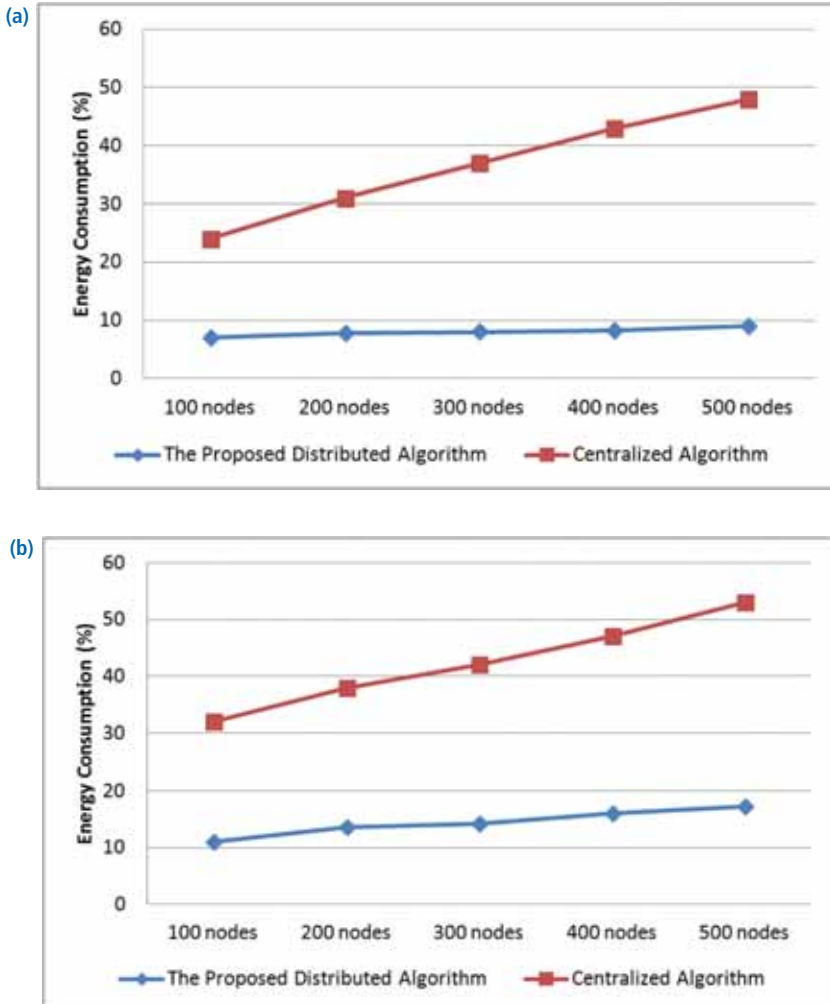


Figure 6: Comparisons of energy consumption for simulation times of: (a) 100s and (b) 200s

Algorithm 1: Distributed image compression algorithm

1. if I am a **camera node**
2. if QUERY msg is received
3. if I have required data
4. **send** REQUEST msg to closest cluster head
5. if REPLY msg is received from the cluster head
6. **partition** the image data into rows
7. **send** them to member nodes
8. if I am a **cluster head** node
9. if REQUEST msg is received
10. **send** REPLY msg to the camera node
11. if Wavelet Transformed (rows) image data is received
12. **combine** intermediate results
13. **partition** data into columns
14. **send** them to member nodes
15. if Wavelet Transformed (columns) image data is received
16. **combine** intermediate results
17. **select** LL part of the image data
18. **distribute** it to member nodes
19. if I am a **member node**
20. if image data is received
21. **process** Wavelet Transform on the image data
22. **send** intermediate results to head of the next cluster

Simulations

We compared the proposed algorithm with the centralized algorithm in terms of image quality, total energy consumption and system lifetime parameters. Image quality is measured by calculating the peak signal-to-noise ratio (PSNR). Comparisons are made on a standard 256 x 256 Lena image. Nodes are located

REFERENCES

- [1] C. G. Panayiotou, D. F. Michalis, P. Michaelides, "Environmental Monitoring Using Wireless Sensor Networks", University of Cyprus Department of Electrical and Computer Engineering Discussion Paper
http://www.eng.ucy.ac.cy/christos/Papers/PFM_WMCCS.pdf
- [2] H. Wu, A. A. Abouzeid, "Energy efficient distributed image compression in resource-constrained multi-hop wireless networks", *Computer Communications*, 2005, Vol. 28, pp: 1658-1668.
- [3] F. Tian, J. Liu, Enyan S., C. Wang, "An Energy Efficient and Load Balancing Distributed Image Compression Algorithm in WMSNs", *Elsevier Procedia Engineering*, 2011, Vol 15, pp: 3421-3427.
- [4] Q. Lu, W. Luo, J. Wang, B. Chen, "Low-complexity and energy efficient image compression scheme for wireless sensor networks", *Computer Networks*, 2008, Vol. 52, pp: 2594-2603.
- [5] E. Sun, X. Shen, H. Chen, "A Low Energy Image Compression and Transmission in Wireless Multimedia Sensor Networks", *Procedia Engineering*, 2011, Vol. 15, pp: 3604-3610.
- [6] M. Nasri, A. Helali, H. Sghaier, H. Maaref, "Adaptive image compression technique for wireless sensor networks", *Computers and Electrical Engineering*, 2011, Vol. 37, pp: 798-810.

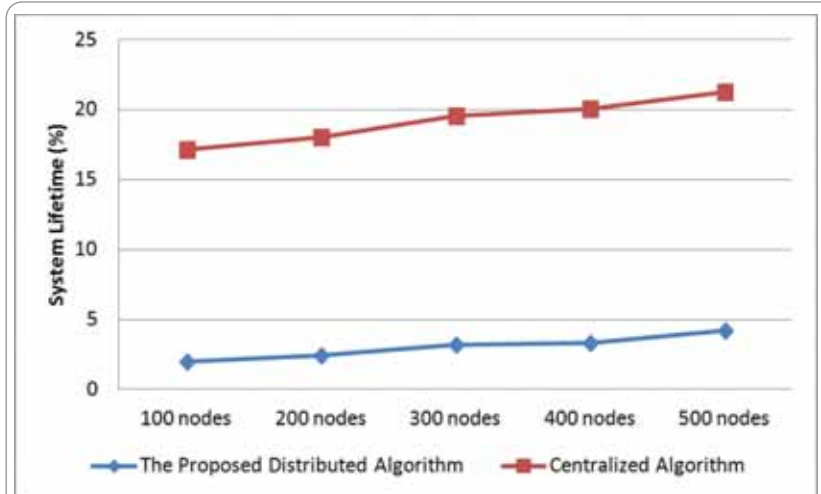


Figure 7: Comparisons of system lifetime for 100s

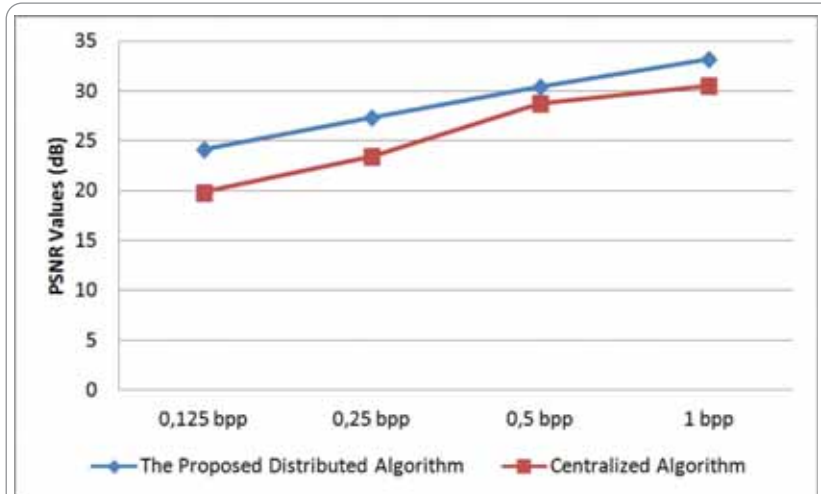


Figure 8: Comparison of image quality at different compression ratios for Lena

randomly in a 5100 x 1200m area. Each node has a 250m communication range and the initial energy of a node is set to 100J. Simulations are made for 100, 200, 300, 400 and 500 nodes. The transmission power of a node is 0.660W and its receiving power 0.395W. We also compared the performance of the algorithm for different simulation times such as 100, 200, 300, 400 and 500s.

Figure 6 shows a comparison of the proposed and centralized algorithms for different number of nodes and simulation times in terms of energy consumption. It can be seen that as the total numbers of nodes and simulation times increase energy consumption also increases in both algorithms, however the proposed algorithm performs better than the centralized algorithm in all cases.

Figure 7 shows a comparison of algorithms for different total numbers of nodes in terms of system lifetime. It can be seen that system life increases as the number of nodes increases, and that the proposed algorithm performs better than the centralized algorithm for any number of nodes.

Figure 8 shows a comparison of algorithms for different compression ratios in terms of image quality. Clearly, for all compression ratios the proposed algorithm performs better than the centralized algorithm. ●

Economy oscilloscopes redefined.

InfiniiVision 2000 X-Series

70 to 200 MHz

New memory depth up to 1 Mpts

New serial decode options*

New 5-year warranty

Starting at ~ €1,000**



InfiniiVision 4000 X-Series

200 MHz to 1.5 GHz

12.1-inch touch screen

InfiniiScan Zone touch triggering

Update rate to 1 million wfms/s

Memory depth up to 4 Mpts

InfiniiVision 3000 X-Series

100 MHz to 1 GHz

8.5-inch display

Update rate to 1 million wfms/s

Memory depth up to 4 Mpts



Receive more
oscilloscope bandwidth
for FREE!



www.agilent.com/find/bandwidthpromo

Offer Ends:
March 31st, 2014

Oscilloscopes Redefined. With its brilliant 8.5-inch screen, fast update rate, full upgradability and 5-in-1 instrument integration, the Agilent 2000 X-Series oscilloscope is already first in class. Now with more memory depth, new serial decode options and 5-year warranty, it's accelerating ahead. Experience the complete InfiniiVision line for oscilloscope features and performance you need at prices that will surprise you.

**Agilent and our
Distributor Network**
Right Instrument.
Right Expertise.
Delivered Right Now.

**Buy from an
Authorized Distributor**
www.agilent.com/find/distributors

**See the InfiniiVision
X-Series oscilloscopes**
www.agilent.com/find/Xoscilloscope



HOW TO CHOOSE THE RIGHT TEMPERATURE SENSOR FOR YOUR PROJECT

BERND HEIM AT AVNET ABACUS EXPLAINS THE TECHNOLOGIES BEHIND VARIOUS TYPES OF TEMPERATURE SENSORS AND HOW THESE TECHNOLOGIES DETERMINE THE SENSORS' PERFORMANCE

Knowing your next project will need to measure temperature is one thing, but knowing how best to do it is quite another. Understanding the nature of what you are trying to measure is key: is it a gas, liquid or solid; do you require an ambient, surface or core temperature; do you need an instantaneous reading or one averaged over a specific time interval; what is the temperature range to be covered and what accuracy/resolution is required? All these things need to be understood before an appropriate temperature sensor can be selected.

Temperature is a basic physical property and methods to measure it in some kind of standardised way have been around since Roman times. Even more modern approaches go back several centuries, as scientists devised equipment that could utilise the property of a material, such as the expansion of mercury, to provide a calibrated measurement of temperature. The concept of a temperature scale is now familiar to us all, starting with the Fahrenheit scale, named after its creator, and introduced early in the 18th century. Anders Celsius developed his equally familiar scale later that century. These scales are both defined by the temperature at which water freezes (32°F or 0°C) and boils (212°F or 100°C).

Slightly more recently, in the mid-19th century, Lord Kelvin proposed his scale based on the idea of an absolute zero temperature where all molecular motion stops. The Kelvin scale, with units simply denoted as K, has since been adopted as the SI unit for temperature, but is easily converted from Celsius by adding 273 (or more precisely 273.15), i.e. 0°C = 273K, or conversely 0K = -273°C.

Here, we are concerned with the electrical measurement of temperature, which is dependent on devices that exhibit an electrical characteristic that varies predictably with temperature. This article will examine the wide range of temperature sensing products available today to understand how the different technologies relate to our design considerations and what makes one product better than another for a given application. We will cover thermistors, thermocouples, resistance temperature detectors (RTDs) and infrared thermopiles and will highlight specific product examples from manufacturers such as GE Sensing, AVX, Measurement Specialties and Vishay.

Thermistors

The name thermistor derives from 'thermal resistor', which clearly refers to its nature as a sensing element whose resistance changes in proportion to temperature. Depending on material characteristics, thermistors can exhibit a positive or negative temperature coefficient (PTC or NTC). PTC thermistors, whose

resistance increases with increasing temperature, are typically used as heating elements or in circuit protection applications – because the increasing resistance limits current, which in turn prevents thermal runaway.

Thermistors used for temperature measurement and more rigorous control applications are all NTC types but even these come in a broad range of designs, including leaded, leadless and surface mount packages, as well as various screw-in, screw-on, clamp and other probe formats. Such devices are relatively inexpensive, offering high sensitivity and accuracy with operation over a wide temperature range, spanning -200°C to +500°C, depending on the type. They address a broad spectrum of applications from automotive, medical and industrial through to white goods and other consumer products. Typical examples of domestic appliances that use thermistors for temperature control include refrigerators, toasters, electric heating blankets, washing machines and water heaters. Examples in automotive include coolant sensors, emission controls, climate control and various engine block, air intake and transmission oil temperature sensors.

Typical leaded thermistors are either glass or resin encapsulated

Figure 1: BR42 Series glass-encapsulated bead thermistor from GE Sensing



Figure 2: A thermocouple probes from Measurement Specialties



with resin types having a more limited operating range from -55°C up to $+125^{\circ}\text{C}$, while glass types extend up to $+300^{\circ}\text{C}$ and tend to be physically smaller, have faster thermal response times and may offer tighter tolerances. Surface mount (SMD) thermistors are also restricted to a narrower temperature range, down to -55°C and up to $+150^{\circ}\text{C}$.

Figure 1 shows a larger size (2.4mm long x 1.16mm diameter) glass-encapsulated bead thermistor from GE Sensing – this series offers temperature options from -80°C to $+300^{\circ}\text{C}$, nominal 25°C resistance values from 30Ω to $20\text{M}\Omega$, platinum alloy leads and a thermal response time of 4.5s in still air or 140ms when plunged into water. There's an NB12 series of SMD thermistor from AVX, which provides nickel barrier termination, operation from -55°C to $+150^{\circ}\text{C}$ and a thermal response time of 5s. Use in battery packs and switch mode power supplies are among the applications claimed for the NB12 devices.

Thermocouples

A thermocouple is formed by contact between two conductors made from different materials and generates a voltage when the junction is heated (or cooled) relative to the reference temperature at the other end of the conductors. The magnitude of the voltage generated is proportional to the difference in temperature between the 'hot junction' and the reference, or 'cold junction'. While the 'cold junction' could be maintained at a known reference temperature this is generally not convenient in most applications. Instead the temperature of this junction can be measured with another temperature sensing device such as a thermistor or RTC (see next section).

Thermocouples are inexpensive and can measure temperatures of over 1000°C , which makes them an attractive solution for industrial applications such as monitoring the temperature of kilns and the exhausts of gas turbines, diesel engines, etc. Different temperature ranges and sensitivities are achieved through the use of different alloy pair types for the conductors. Type K is the most common with chromel (90% nickel, 10% chromium) and alumel (95% nickel, 2% manganese, 2% aluminium, 1% silicon) conductors, providing an operating range from -200°C to $+1350^{\circ}\text{C}$ with a sensitivity of $41\mu\text{V}/^{\circ}\text{C}$. The main limitation of thermocouples is accuracy, which is unlikely to be better than 1°C .

Thermocouples are usually supplied as probe assemblies, which contain the sensing junction in a protective metal or ceramic jacket attached to a standard connector as shown in Figure 2. This mineral insulated thermocouple, from Measurement Specialties, offers high corrosion resistance with different sheath materials and is available with K, J, T or N type conductors, supporting operation from -40°C to $+1000^{\circ}\text{C}$.

Resistance Temperature Detectors (RTDs)

Resistance temperature detectors (RTDs) are temperature-

sensing devices based on metal elements whose resistance varies linearly with temperature. All metals satisfy this basic criteria but the ideal material for an RTD is one with a high resistivity that also has a high melting point and can withstand the effects of corrosion. Nickel or nickel alloy are used in more cost-sensitive consumer applications but these materials have a limited temperature range.

The majority of RTDs use platinum as the sensing element, which is either implemented using a traditional wirewound construction or produced with thin-film technology where a thin layer of platinum is deposited on a substrate.

Wire-wound coil type RTDs are usually packaged in glass or ceramic tubes, while thin-film types are either provided with protective coatings and offered in leaded or SMD configurations, as illustrated by the Vishay

A thermocouple is formed by contact between two conductors made from different materials and generates a voltage when the junction is heated (or cooled) relative to the reference temperature at the other end of the conductors

products in Figure 3, or encapsulated in epoxy plastic SOT-23 transistor-style SMD packages as used by Measurement Specialties. RTDs are also supplied as probe assemblies.

Operating temperature ranges depend on package type/construction, with ceramic wirewound types offering the widest range from -200°C to 1000°C . Resistance values at 0°C (R_0) are typically a few hundred ohms but extend to 10k for some types with customised solutions from some vendors.

Infrared (IR) Thermopiles

Infrared thermopiles are primarily used for contactless temperature measurement, measuring as they do the thermal radiation from the target object. Thermopiles are constructed from a number of thermocouples, usually connected in series to improve temperature sensitivity, and are typically packaged in windowed TO5 or TO18 style packages. Originally quite expensive, the recent implementation of thermopiles using CMOS integrated circuit processes has seen thermopiles replace more costly pyroelectric sensors in many applications, such as medical thermometers as well the spot measurement of temperature in industry.

GE Sensors and Measurement Specialties both offer thermopile sensors for operation from -20°C to $+100^{\circ}\text{C}$. One of the key advantages of this type of non-contact temperature measurement is the response time – these devices have time constants around 20ms.

A Variety Of Sensors

There are a number of materials whose electrical properties vary with temperature. This article has reviewed the technologies developed to provide accurate and reliable temperature measurement devices, spanning temperature ranges from as low as -200°C to in excess of 1000°C . A wide variety of contact and non-contact sensors are commercially available from a number of manufacturers and examples of these have been used to illustrate the differing specifications and package options on offer to suit an equally broad range of application requirements. ●

Figure 3: Vishay's leaded and SMD platinum thin-film RTDs





**RFI / EMI shielding gaskets
& components**

 **Kemtron**
Proven EMC Shielding Performance

www.kemtron.co.uk
+44 (0) 1376 348115 · info@kemtron.co.uk

CUSTOM TEMPERATURE SENSORS

ATC Semitec supply custom temperature sensors using NTC and PTC thermistors, platinum resistance (Pt100/Pt500/ Pt1000) or non-contact, infra-red sensing thermopile technology.

Cost-effective IP68 rated sensors ensure absolute moisture integrity in ground water or refrigeration applications, whilst our fast-response versions can react in under 1 second to temperature change. The wide range of gas boiler temperature sensors provides fast and accurate water temperature control to help provide a comfortable living environment.

Our platinum sensors happily control processes up to 500deg.C and offer long-term stability. Thermopile sensors can react in milliseconds to infra-red energy changes in non-contact applications, both industrial and medical.

Call us today to discuss your latest temperature sensor application.

ATC Semitec Ltd
Tel: 01606 871680 · Fax: 01606 872938
E-mail: sales@atcsemitec.co.uk

www.atcsemitec.co.uk



UP series - open frame SMPS single output with PFC 150W - 500W

Universal ac input with active PFC > 0.90
Low profile U-channel 200W – 500W = 38mm (150W = 33mm)
Output voltage trim range: +/- 10% (fixed on 150W)
Cooling by free air convection (150W to 400W)
No load power consumption < 1W
Protection: OVP; OLP; OTP; SCP
Vibration test: 2G withstand
Temperature range: -20 to +70°C
Approvals: UL; TUV; CE; CB
3 year warranty



Housed in a low-profile U-channel the UP series delivers from 150W to 400W (UP350 = 300W, UP500 = 400W) with free air convection, (UP350 = 350W, UP500 = 500W with fan cooling). Built using 105°C electrolytic capacitors for a long service life, these units are designed for a range of telecom and industrial applications requiring low maintenance and noise. All models have universal ac input, and are available with a single output voltage of 12, 15, 24 or 48Vdc. Safeguards include: short-circuit protection; over-voltage protection; overload protection and over-temperature protection. The 350W and 500W units also feature: active inrush current limiting; remote voltage sensing; remote inhibit function; power OK signal.

Relec Electronics Ltd

Tel: +44 1929 555700 Fax: +44 1929 555701
e-mail: sales@relec.co.uk

www.relec.co.uk

Design solutions for design engineers

HIGHLY RELIABLE ENCAPSULANTS FOR MICROELECTRONICS DEVICES

NEWLY DEVELOPED ENCAPSULANTS HELP PROTECT SENSORS, ACTUATORS AND SEMICONDUCTORS FROM THE HARSHNESS OF THEIR OPERATING ENVIRONMENTS.

BY **DR TOBIAS KÖNIGER**, PRODUCT MANAGER AT DELO INDUSTRIAL ADHESIVES



High-reliability encapsulants used in packaging of microelectronic components continue to play an increasingly important role. Electronic components tend to be subjected to aggressive environmental conditions, including fuels, oils, vibration and extreme temperatures, so enhanced encapsulants based of anhydride-curing epoxy resins have been developed for further protection. They offer fast and stable production processes, thanks to optimized flowing and dispensing properties and various curing options.

Encapsulation is mainly found in chip-on-board (COB) technology. With this method, semiconductor chips or sensor elements are completely or partially encapsulated on a printed circuit board, so the encapsulant protects the

assemblies from thermal and mechanical stress and other aggressive environmental factors. Further application areas include sensors and actuators, such as sealing of oil pressure sensors in engine compartments.

Microelectronic Packages With Special Properties

The encapsulants' materials are based on epoxy resins that contain organic anhydrides as the hardener component. New materials with unique properties have been created by mixing base resins with specific properties, using adhesive agents and adding fillers. The special ring structure of the anhydride hardeners allows extremely narrow polymer crosslinking, resulting in a glass transition temperature of 180°C.

These polymers also have low coefficients of thermal

	DELOMONOPOX GE725	DELOMONOPOX GE785	DELOMONOPOX GE730	DELOMONOPOX GE765
Application area	fill	dam	glob top	glob top
Color	black			
Filler content [weight %]	65	68	65	67
Viscosity [mPas]	6,500	135,000	9,000	19,000
Processing time [h]	48			
Curing conditions until final strength	4,5 h @ +100°C 1,5 h @ +125°C 20 min @ +150°C			
Tensile strength [MPa]	50	55	60	60
Elongation at tear [%]	0.5	0.5	0.7	0.7
Young's modulus [MPa]	9,800	11,000	9,000	9,000
Glass transition temperature [°C]	+178	+182	+179	+186
Coefficient of thermal expansion [ppm/K]	25	22	24	18
Water absorption [weight %]	0.1			

Table 1: Property overview of the new encapsulants

expansion (between 18 and 25ppm/K), so only small amounts of oxygen and chemicals can diffuse into the material, even at elevated temperatures. This results in low water absorption of 0.1 weight % and very high resistance to heat and chemicals. The basic product properties are shown in Table 1.

Mechanical Properties

Figure 1 illustrates the excellent mechanical properties after thermal aging at 150°C and even at 180°C for 1000h using one encapsulant as an example. The figure shows the percentage changes in Young's modulus, tensile strength and elongation at tear, related to the initial value. The differences are very small and prove the high stability of the mechanical values in harsh conditions, that means under temperature stress at 150°C and 180°C, respectively, as usually required for electronic components, for example sensors and actuators close to the engine. The mechanical properties remain at a nearly unchanged high level, even under permanent temperature stress at 180°C.

Figure 2 demonstrates the universal chemical resistance of the new adhesives. Bonded aluminum compression shear specimens were tested by storing them in chemicals like Ad Blue, ATF gear oil, motor oil or diesel fuel for 100h and 1000h at room temperature.

These storage conditions are based on the requirements of automotive production, which assume a high quality level of the materials used in cars. The results are above 80% of the initial value, even after storing them for 1000h, which shows the high resistance to these aggressive liquids.

Furthermore, the materials adhere very well to the materials frequently used in electronics and microelectronics, such as FR4 or technical plastics like PA 6.6, PPS or LCP.

In Figure 3, the exceptionally high strengths of 40MPa and up achieved on FR4 stand out from the other values. The values achieved on technical plastics, such as PA, PPS and PBT are also very high and range from 15-27MPa. Even on LCP, which is very difficult to bond, values of at least 10MPa can be achieved.

Processing Properties

The processing properties were specifically designed and optimized for efficient use in microelectronic production.

The flow behaviour of the products plays an important role as well for optimal dispensing and fast processes. The new products, designed as Dam&Fill for the Chip-on-Board (COB) technology, can be processed wet-on-wet. This implies that intermediate curing of the dam before

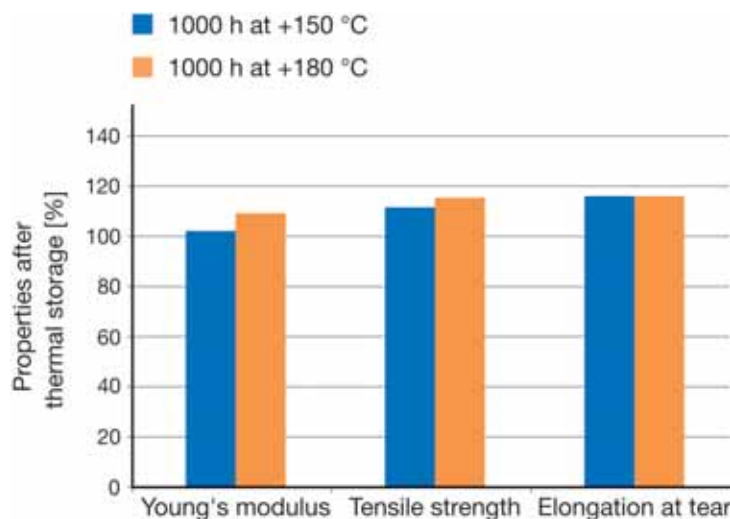


Figure 1: The mechanical properties of DELOMONOPOX GE730 are only marginally influenced by thermal aging (initial value without aging)

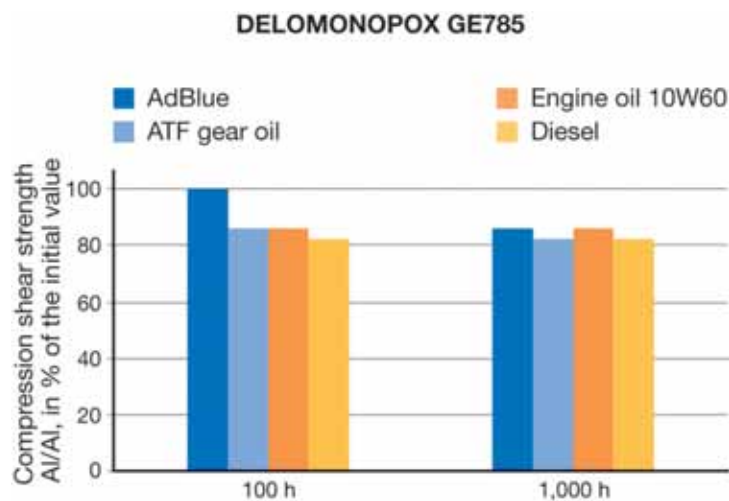


Figure 2: Chemical resistance of the new adhesives using DELOMONOPOX GE785 as an example. The figure shows the relative compression shear strength related to the initial strength under the influence of diverse aggressive liquids

dispensing the fill is not necessary, which shortens the process time significantly. The dam does not flow under temperature influence and forms a flow barrier for the low-viscosity fill. Therefore, numerous dispensing patterns can be reliably dispensed, so the flow behaviour is also excellent for partial encapsulation, as often required by sensor applications (Figure 4)

The dam adhesives allow a particularly narrow but nevertheless stable wall. Several walls can be stacked that way (Figure 5). This permits a high degree of freedom regarding the shape of the encapsulation. The dams can be dispensed in succession without intermediate curing. Afterwards, the complete encapsulation including fill is cured

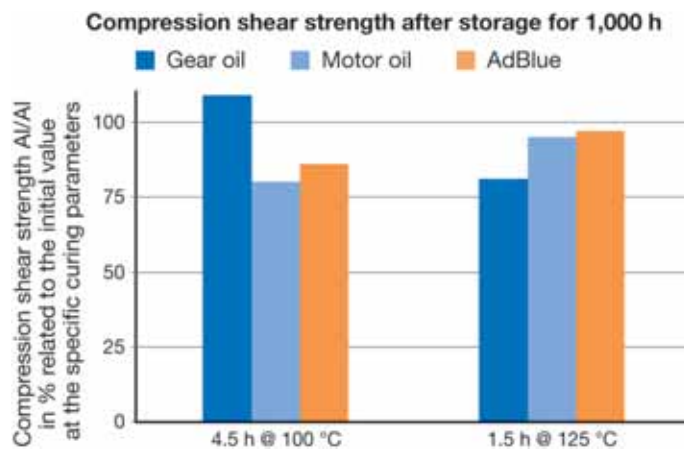


Figure 3: Compression shear strength as an indicator of the universal adhesion of the new encapsulants to many substrate materials



Figure 4: For partial encapsulation, only parts of the chips are covered by adhesive. In this case, it is particularly important that the adhesive cures at its intended position without flowing

in one step with heat. The innovative encapsulants allow the customer to essentially improve his production capacity as the intermediate curing steps are eliminated.

Besides the Dam&Fill adhesives, the encapsulant range also includes two glob top encapsulants (Figure 6). Depending on the application, the user can select between a low-viscosity adhesive and a higher-viscosity product. Partial encapsulation is also possible with the glob top encapsulants thanks to their optimized flow behaviour.

Optimized Dispensing

Another benefit for production is the long processing time of 48h at room temperature. Normally, an increase in viscosity by 50% over the initial value is used as reference criterion for the processing time. This is quite disadvantageous for the user as the dispensing parameters, for example pressure, must be adjusted in accordance with the viscosity increase to achieve a uniform dispensing pattern. The viscosity of the new products does not show any increase over the entire processing time of 48h at room temperature, enabling a very even dispensing pattern. As their viscosity deviates only slightly from the initial value, it is not necessary to readjust the dispensing parameters during processing.

Especially in automotive production, fast processes with dissimilar materials are a basic precondition. The variable heat-curing parameters represent another benefit of customer-friendly processing. Encapsulants can be cured quickly at 150°C within 20 minutes. Nevertheless, curing is also possible at moderate temperatures of 125°C within 1.5h or 100°C within 4.5h. As seen in Figure 8, the chemical resistance is not significantly influenced by the curing parameters. The user can then design the process flexibly.

Reliability Qualification

Functionality of components encapsulated as glob top or Dam&Fill was maintained even after aggressive tests like storage at 85°C/85%-relative-humidity for 3000h, 1000 cycles of temperature shocks between -40°C and +150°C, three flows in lead-free reflow solder at 260°C, and JEDEC Level I.

A number of special Daisy Chain Packages (5mm x 5mm, 25µm Au wire, FR4) were subjected to testing for internal qualification. The chips, bonded to an FR4 PCB were encapsulated, with the new glob top and Dam&Fill adhesives, followed by testing them for functionality and test-specific conditioning. Using the reliability classification JEDEC MSL I,



Figure 5: For "dam stacking", several adhesive beads are stacked and form a kind of wall. The volume within the wall can be completely filled with the low-viscosity encapsulant (fill). Afterwards, both compounds are cured in just one step

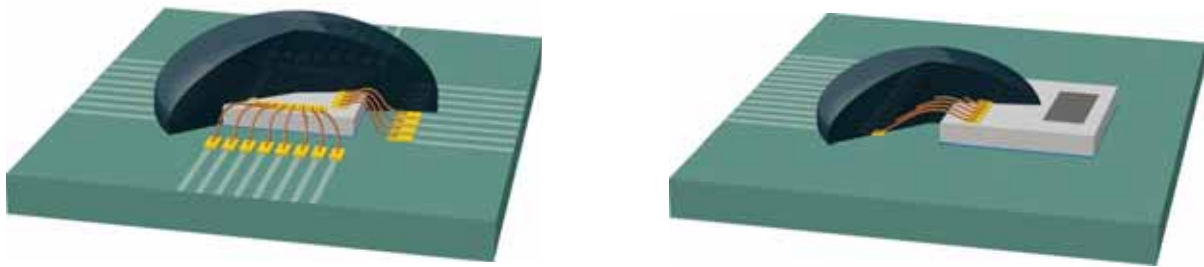


Figure 6: The optimized glob top encapsulants can be used for full and partial encapsulation: on the left is a full glob top, whereas on the right a partial glob top

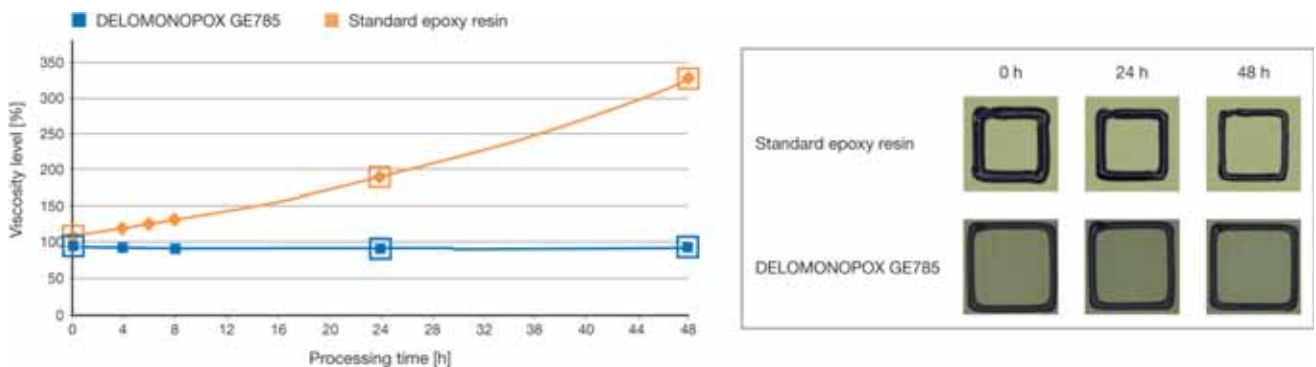


Figure 7: Change in viscosity of DELOMONOPOX GE785 within the processing time related to the initial value. Compared to a standard product, the dispensing pattern remains unchanged at constant dispensing parameters in dependence of the processing time

the components were initially dried at $125 \pm 5^\circ\text{C}$ in an air convection oven for 24h; then, they were conditioned at 85°C and 85% relative humidity for $168 \pm 5\text{h}$. After these preparations, the components were subjected to reflow stress three times. Their functionality was checked after each flow. The result verifies the excellent properties of the products, as all tested components functioned perfectly after being stressed.

Reliability

Reliable encapsulation of microelectronics that must function under extreme conditions presents great challenges for adhesives. The new encapsulants combine outstanding properties, such as chemical resistance, mechanical properties, excellent adhesion, optimized dispensing and flowing, and variable curing parameters. Thanks to this successful development, production processes can be designed in a much more flexible and efficient way. This helps users reduce production costs and boost output, while achieving the highest product quality. ●

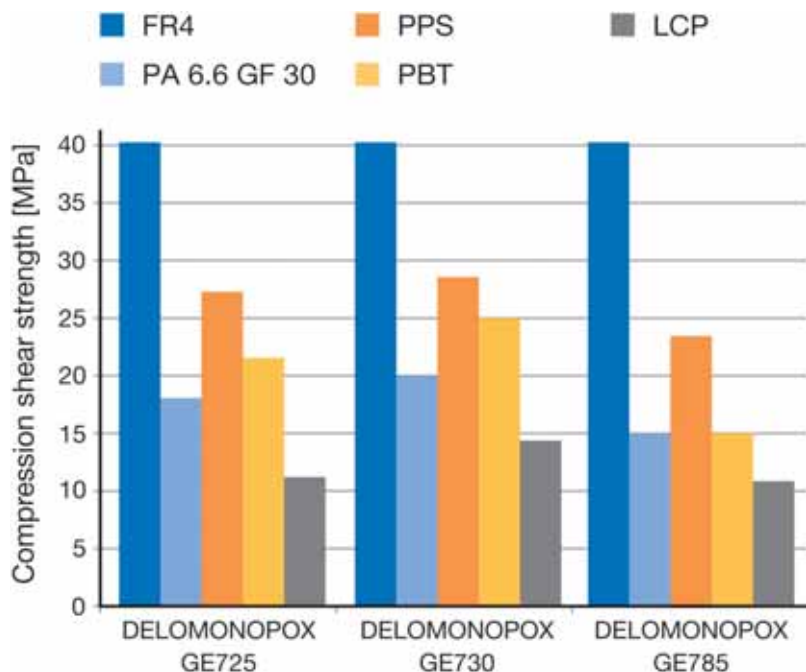


Figure 8: Chemical resistance of DELOMONOPOX GE725 at dissimilar curing parameters



JIHONG PANG FROM THE COLLEGE OF MECHANICAL AND ELECTRONIC ENGINEERING AT WENZHOU UNIVERSITY AND **GENBAO ZHANG** FROM THE COLLEGE OF MECHANICAL ENGINEERING AT THE CHONGQING UNIVERSITY IN CHINA PRESENT AN ABSTRACT INTELLIGENT FAULT DIAGNOSIS SYSTEM (IFDS) WITH MULTIPLE CHARACTERISTIC PARAMETERS FOR QUALITY MONITORING AND CONTROL OF ELECTROMECHANICAL PRODUCTS, BASED ON A SELF-ORGANIZING MAP (SOM)

THIS REGULAR FEATURE COVERS CHINESE RESEARCH AND DEVELOPMENT

An Intelligent Fault Diagnosis System For Quality Monitoring And Control Of Electromechanical Products

Quality monitoring and control of electromechanical products is of interest to companies worldwide. As such, it has become increasingly important to measure multiple parameters during the manufacturing process and over the past decade there has been a move towards intelligent systems and greater automation of fault diagnosis for this purpose.

Quality monitoring and control of products can be implemented by using technology based on the Abstract Intelligent Fault Diagnosis System (IFDS), which is gaining widespread acceptance; see its framework in Figure 1.

IFDS Based on SOM

The process of building an intelligent system consists of problem selection and data acquisition, representation, programming, testing, evaluation and so on. We focused on two areas: collecting the data and building the IFDS.

Our IFDS solution is based on the self-organizing map (SOM) algorithm. A SOM neural network is an effective tool for analysis of multidimensional data. After SOM has been trained with a group of example faults, many faults can be diagnosed based on this type of neural network. As a good neural network tool, SOM has been widely used for fault analysis and forecasting in various

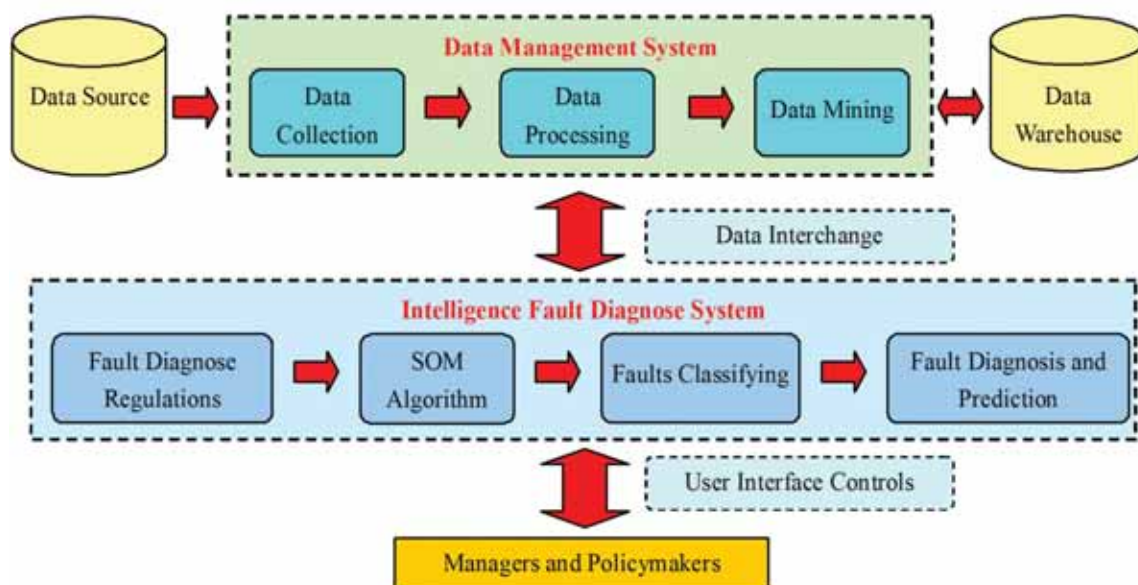


Figure 1: Framework of intelligent fault diagnosis system

THE GIFT OF INVENTION



DESIGNSPARK MECHANICAL

At RS Components we love helping engineers create world-changing products.

Our dedication to innovation and progress is why we want every designer to enjoy the benefits of world-class design tools.

DesignSpark Mechanical is a powerful, easy to learn 3D modelling software. It provides a highly intuitive user experience, helping you create great concepts faster than ever before.

DOWNLOAD DESIGNSPARK MECHANICAL FOR FREE at www.designspark.com



Discover your next invention with DesignSpark Mechanical



**DESIGNSPARK
MECHANICAL**

BROUGHT TO YOU BY





engineering applications, but also in medicine, economics, mathematics, physics and chemistry among others.

SOM's Learning Algorithm

The learning algorithm for the SOM is as follows:

By using normalization data, we can easily train the SOM neural network with competitive learning. Secondly, we will compute the Euclidian distance between two vectors. The Euclidian distance of an input vector can be calculated as:

$$D_j = \|Y - W_j\| = \left(\sum_{i=1}^n (x_i(k) - w_{ji}(t))^2 \right)^{\frac{1}{2}} \quad (1)$$

where $Y = (i_1, i_2, i_n)$ denotes an input vector, and $W_j = (w_{j1}, w_{j2}, w_{jn})$ denotes the weight vector of the j th neuron. The numbers of new neural nets of minimum distance can be described as:

$$D_k = \min(D_j) \quad (2)$$

The weight of adjacent vectors can be calculated as:

$$w_{ij}(k+1) = w_{ij}(k) + \alpha(k)(y_i(k) - w_{ij}(k)) \quad (3)$$

where $\alpha(k)$ is a function that decreases with time.

Finally, we can get the weight vectors from the following:

$$E_{ow} = h(\min_j \|Y - W_j\|) \quad (4)$$

where E_{ow} is between -1 and 1.

Intelligent Fault Diagnosis Example

Our case study examines quality monitoring and control procedures developed in the manufacturing industry. An experimental application of this monitoring process to the NC rotary table of a computer numerical control (CNC) machining centre is described here (see the setup in Figure 2). In addition, the computer-based data can be used to monitor multiple parameters. Once the control trials have been completed, the data for each parameter is automatically saved.

The intelligent fault diagnosis device of the NC rotary table was developed based on the IFDS framework of Figure 1. The system has to be connected to a local computer, as well as other remote computers on the same network.

The computer automatically runs the IFDS program. The multiple characteristic parameters (CP) of the NC rotary table include positioning accuracy (CP1), coaxiality of bearing and revolution body (CP2), gear backlash (CP3), coaxiality of bearing and crankset (CP4), shaft axial play of NC rotary (CP5), circular run-out error (CP6), lateral deflection of NC rotary (CP7), coaxiality of bearing and axle (CP8), cleaning shaft and oil hole (CP9).



Figure 2: Intelligent fault diagnosis device of an NC rotary table

After the composite variables and normalization analysis were used to reduce this data, the normalized data can be determined based on statistical methods. All nine CPs of the SOM neural network diagnosis process are shown in Table 1.

The numerical simulation in the time domain can be determined using the SOM arithmetic with a MATLAB software tool. With the Euclidian distance between two vectors computed by the SOM method, we can see the SOM neighbour weight distances of the fault samples in Figure 3.

In order to explain the weight change of the characteristic parameters, this project takes the SOM weight planes of 16 test data points in the case study. By applying clustering analysis to the SOM sample hits of such data, the results verify its accurate classifications, more so than using other methods. Once the configuration of the intelligent system is complete and saved, the data processing location is added to the quality monitoring and control. The SOM weight positions of the fault samples are shown in Figure 4.

The output of this fault classifier is the result of nine CPs as in $R = [20, 15, 1, 33, 95, 56, 100, 91, 8]$. As a result, the fault diagnosis results are classified correctly, which confirms the feasibility and accuracy of the proposed method. Based on IFDS, there is a great improvement in the efficiency and reliability, leading to a reduction of post fault-diagnosis testing. Moreover, the IFDS is inexpensive to design and can be easily networked to provide convenient and fast communications with an integrated database on a larger computer or cloud.

The next step was to monitor and control product quality with IFDS based on a trained SOM neural network. By using a test swatch, the in experimental tests' faults diagnostic rate is above 93%, further confirming the validity of this algorithm.

A New Way Forward

Many manufacturing companies around the world are experimenting with fault diagnosis technology and new solutions continue to emerge. The purpose of this article was

Nuremberg, Germany
25 – 27.2.2014

Register now and make
sure of your tickets!
embedded-world.de

embedded world 2014 Exhibition & Conference ... it's a smarter world

Innovation summit

The world's biggest event for embedded technologies invites you.
This is where the international embedded community sets the
trends for tomorrow's technology – so be there, make contacts
and expand your networks!

Media partners

elektroniknet.de

computer-automation.de

energie-und-technik.de

karriere-ing.de

Markt & Technik

Elektronik

**Elektronik
automotive**

**ENERGIE
& TECHNIK**

**COMPUTER
AUTOMATION**

MEDIZIN & elektronik

**DESIGN &
ELEKTRONIK**
KNOW-HOW FÜR ENTWICKLER

Exhibition organizer

NürnbergMesse GmbH

Tel +49 (0) 9 11.86 06-49 12

visitorservice@nuernbergmesse.de

Conference organizer

WEKA FACHMEDIEN GmbH

Tel +49 (0) 89.2 55 56-13 49

info@embedded-world.eu

NÜRNBERG MESSE

Vector Network Analyzer Bode 100



All in one:

- Gain Phase Meter
- Vector Network Analyzer
- Frequency Response Analyzer
- Impedance Analyzer

Wide frequency range: 1 Hz - 40 MHz

High accuracy of results

Easy data processing & data sharing

Portable - compact lightweight design

Automation Interface

**Measure transfer functions
from 1 Hz to 40 MHz!**

More at www.omicron-lab.com

Smart Measurement Solutions



to present an IFDS that will enable business managers to better monitor and control the quality of electromechanical products. This approach to product quality monitoring and control will vary with progress from the experimental stage to the engineering application stage.

We presented an illustrative example of the use of IFDS with

multiple characteristic parameters and in the future we expect to see great improvements in this area with further improvements in technology. ●

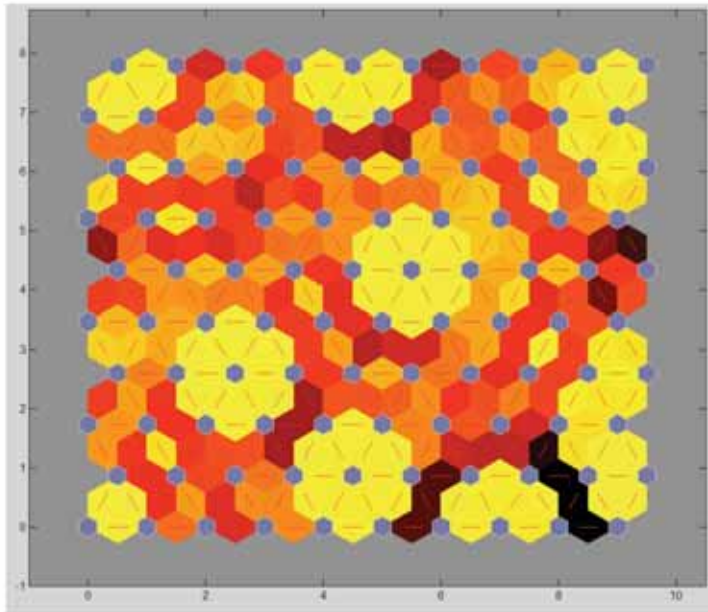


Figure 3: SOM neighbour weight distances of the fault samples

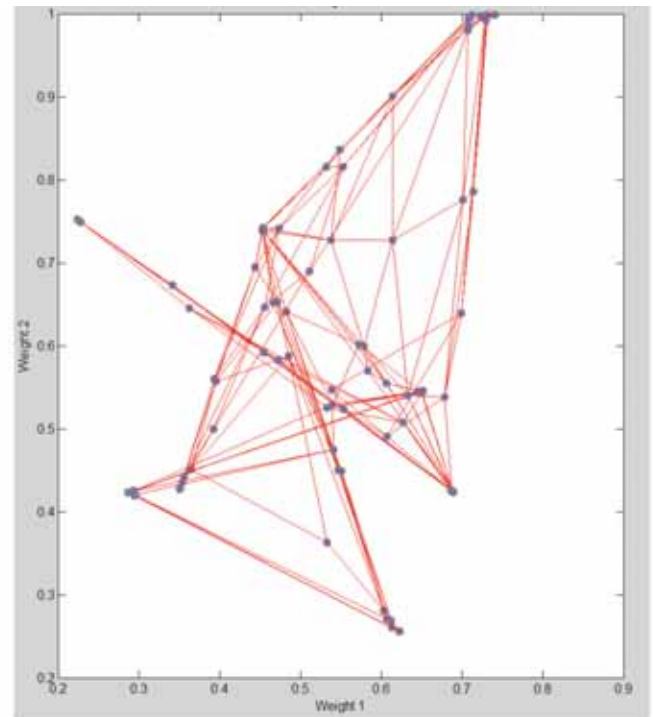


Figure 4: SOM weight positions of the fault samples

CP1	CP2	CP3	CP4	CP5	CP6	CP7	CP8	CP9
0.6225	0.6521	0.2235	0.6895	0.7123	0.4523	0.3502	0.7412	0.2852
0.2556	0.5467	0.7524	0.4236	1.0000	0.7412	0.4278	1.0000	0.4238
0.5348	0.4037	0.1258	0.5072	0.4123	0.3542	0.5017	0.6341	0.3627
0.2834	0.3679	0.6782	0.3674	0.3216	0.2527	0.7236	0.5027	0.6275
0.7831	0.3546	0.4328	0.1257	0.4257	0.4269	0.4235	0.6341	0.5634
0.7563	0.6524	0.4675	0.6398	0.2852	1.0000	0.6543	0.0453	1.0000
0.2057	0.6247	0.5023	0.4562	0.4536	0.5124	0.8243	0.7024	0.2385
0.6482	0.3254	0.1254	0.4253	0.7256	0.7501	0.8123	0.3621	0.5368
0.3546	0.8324	0.5126	0.7524	0.1023	0.3457	0.4131	0.5076	0.8624
0.5247	0.5417	0.6378	0.3265	0.1204	0.4562	0.5017	0.5387	0.7569
1.0000	0.5368	0.1286	0.2546	0.8369	0.4351	0.1726	0.6385	0.6354
0.8652	0.5694	0.6725	0.8523	0.2456	0.3562	0.2637	0.7523	0.7521
0.3354	0.7368	0.8634	0.7326	0.4368	0.6542	0.2675	0.5246	0.6387
0.6051	0.5242	0.8022	0.7561	0.6532	0.8123	0.7242	0.8022	0.4386
0.7343	0.8031	0.3259	0.4078	0.3124	0.4548	0.6018	0.7342	0.5622
0.4475	0.4257	0.6255	0.5254	0.8251	0.6507	0.9125	0.9625	0.7364

Table 1: Normalized data of the SOM neural network diagnosis process

This project was supported by the National Natural Science Foundation, China (No.71301120, No.50835008), the Provincial Natural Science Foundation, Zhejiang, China (No.LY13G010002), the Opening Laboratory Project, Wenzhou University (No.13SK58A), and the Students Scientific Research Subject of 2013, Wenzhou University (No.269).

01279

Credit Card
Sales

467799

Ho! Ho! Ho! Christmas 2013 is on it's way but
DON'T PANIC!!
We have some fantastic gift ideas for young (and old) enquiring minds

Electronic Project Labs

An electronics course in a box! All assume no previous knowledge and require NO solder. See website for full details



30 in ONE - £17.95
Order Code EPL030



130 in ONE - £49.95
Order Code EPL130



300 in ONE - £79.95
Order Code EPL300



500 in ONE - £179.95
Order Code EPL500



Robot Sensor - £21.95
Order Code EPLR20



Digital Recording Laboratory - £29.95
Order Code EPLDR



AM/ FM Radio Kit - £9.95
Order Code ERKAF



Short Wave Kit - £9.95
Order Code ERKSW



Crystal Radio Kit - £8.95
Order Code ERKC



Electronic Bell - £6.95
Order Code EAKEB



Electronic Motor - £6.95
Order Code EAKEM



Generator - £6.95
Order Code EAKEG



Room Alarm - £4.95
Order Code EAKRA



Hand Held Metal Detector - £7.95
Order Code ELM DX7



Metal Detector - £7.95
Order Code ELMD

Robot & Construction Kits

Future engineers can learn about the operation of electronics, robotics and transmissions systems.



Tyrannomech - £15.95
Order Code C21-601



Robotic Arm - £44.95
Order Code C9895



Crawling Bug with Case - £16.67 - Order Code MK165



Running Microbug - £10.55
Order Code MK127



3 in 1 All Terrain Robot Kit - £38.96
Order Code KSR11

Festive Electronic Project Kits



Riding Santa - £14.66
Order Code MK116



60 LED Multi-Effect LED Star - £14.48
Order Code MK170



Musical LED Jingle Bells - £21.95
Order Code 1176KT



Flashing LED Christmas Tree - £5.16
Order Code MK100

See our website for special offers and even more great gift ideas!



A MONTHLY COLUMN ON TEST AND MEASUREMENT (T&M) ISSUES

Programming Memories In-System With JTAG And An FPGA

BY REG WALLER, EUROPEAN DIRECTOR, ASSET INTERTECH INC

Have you ever tried removing an EEPROM memory device from a circuit board after it's been soldered down? It's not fun and it's something most sane engineers would avoid at all cost. But sometimes you're faced with this kind of predicament.

A great alternative to unsoldering is in-system programming, or programming the device while it's on the board. It turns out that a common test and measurement technique – boundary scan/JTAG – is a handy tool for in-system programming, reaching the full access speeds (at-speed) of memory devices in some applications.

Use Cases

It is fairly common these days that the booting firmware is contained in an EEPROM or flash memory that's connected to the processor via a Serial Peripheral Interface (SPI) bus. Unfortunately, the full complement of a design's firmware is often not available yet when prototypes of a new circuit board design are assembled. So during prototype board bring-up,

when designers are chomping at the bit to verify the board's functionality, the best alternative is usually to load some boot code via an in-system programming method.

Another use case for in-system programming of EEPROMs is during board manufacturing. Some vendors do not program the EEPROM with its firmware until the board is about to be shipped, because the same board will run different versions of the firmware, depending on the application.

At-Speed Programming

Of course, the speed at which a memory device can be programmed is critical. During prototype board bring-up, designers are rarely patient – they want to boot the board right away. And the last thing a manufacturing engineer wants is for in-system memory programming to slow down the assembly line. Nothing slows the assembly line!

Fortunately, there are several different ways to quickly and cost-effectively program on-board memories through the boundary scan/JTAG Test Access Port (TAP) on the board, even though memory devices themselves typically do not include a JTAG interface. You can get around that. In addition, several of these methods start to approach the maximum at-speed limits of memory devices and, in particular, one method involving an SPI Master embedded instrument with associated memory pushes the speed limits for programming SPI memory devices.

Teaming up JTAG and an FPGA

You'll be able to access an FPGA through the board's JTAG TAP, but from there, you'll have to appropriate the FPGA's SPI connection to memory. There are several ways to make the FPGA's JTAG port emulate the SPI bus and its protocols. Some boundary-scan tools provide a

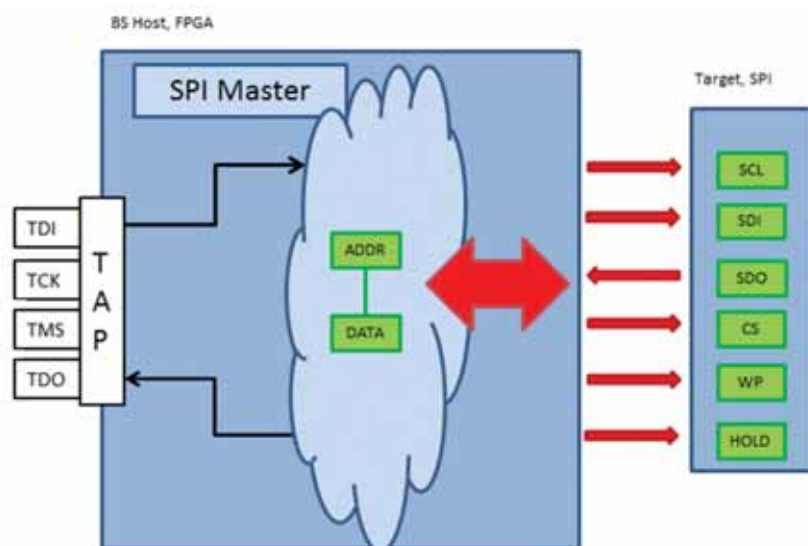


Figure 1: After the boundary-scan tool has loaded the address and data into the SPI Master IP, it can program the connected SPI memory devices at their maximum speeds

complete set of SPI cycle definitions for read and write operations and employ a model-based approach for device programming. This simplifies and significantly shortens the development of programming routines. The programmer doesn't even have to be familiar with the SPI programming protocol to program the memories in-system.

A great alternative to unsoldering is in-system programming, or programming the device while it's on the board

Tradeoffs

The simplest, but slowest method is to just use the FPGA's internal boundary scan chain and output the programming data to the memories. However, the longer the FPGA's internal boundary-scan chain, the slower this method will be. As a result, it is often only used to insert a small amount of data such as a board revision number or software update number.

Another much faster method would require a segment of firmware in the FPGA that would essentially bypass a portion of the chip's internal boundary-scan chain. This could make the programming process hundreds of times faster.

The third method would involve temporarily inserting an SPI Master embedded instrument into the FPGA. Some vendors of boundary-scan tools provide SPI Master intellectual property (IP) code for loading into an FPGA. The SPI Master IP has programmable registers for address and data that are accessed through the FPGA's JTAG TAP. The programming data stream traverses the chip through a network defined by the IEEE P1687 Internal JTAG (IJTAG) standard (Figure 1). After the boundary-scan tool has loaded the address and data into the SPI Master IP, it can program the connected SPI memory devices at their maximum speeds. The programming speed will mostly be determined by the speed of the FPGA's boundary-scan test clock and the throughput of the boundary-scan tool's controller.

Another variation on this theme would be even faster. In this case, the SPI Master embedded instrument will include a memory area, which will usually be implemented as FIFO memory. A cleverly designed SPI Master and a high-throughput boundary-scan controller are typically able to reach the maximum programming speed of the SPI memory device. ●

FURTHER INFORMATION

Additional information on these JTAG-based methods for programming memories in-system is available in an eBook: <http://www.asset-intertech.com/Products/Boundary-Scan-Test/BST-Software/At-speed-SPI-Flash-EEPROM-Programming-FPGA-JTAG>



- 500mW RF power
- Category 1 receiver performance
- Exceptional RX-to-TX switching time (5ms)
- Usable range 5km over open ground
- 256-channel module
- UK 458MHz Industrial & Commercial Telemetry Band & custom frequencies



RADIOMETRIX

www.radiometrix.com



MINIATURE, HIGH-SPECIFICATION OCXO

Choosing a smaller size in oven controlled crystal oscillators (OCXOs) usually means compromising on the performance of the unit. RFX has attempted to minimise the compromise necessary by introducing an SC cut oven controlled oscillator in the industry standard dual in line, fourteen-pin package.

Generally speaking, the smaller the package the greater the difficulty in obtaining good temperature profiling, as there is less isolation to the environment and lower thermal mass to hold stabilities. RFX has overcome this by designing for good thermal isolation combined with high dynamic controller gain, resulting in better than ten parts per billion stability over the temperature range of -40°C to 70°C.

Care has also been taken to ensure that the design does not compromise on noise performance. Careful attention to layout and high power supply noise isolation has resulted in an excellent phase noise performance for the oscillator's size.

www.tfc.co.uk

HAN(R) PUSH/PULL SIGNAL CONNECTOR FOR ALL POWER RANGES

The new Harting Han(R) PushPull Signal connector provides reliable transmission of energy, signals and data over all power ranges, consistently and in a uniform package profile.

The connector has ten contacts, each with a rated current of 5A, for use with conductors with wiring gauges of up to 0.75mm². To ensure EMC interference immunity, the contact inserts are fully screened.

PushPull locking is incorporated for reliable and intuitive connection, and perfect locking is indicated by an audible click.

The PushPull Signal connector can also be used for hybrid applications, with one part of a connector face used for energy transmission and other contacts available for communication signals. PushPull Signal connectors are available in the PushPull 14 and 4 version series in accordance with IEC 61076-6-107.

Han(R) PushPull version 14 is the preferred connector for decentralised automation according to the guidelines of the PROFIBUS user organisation (PNO) and the automation initiative of German automobile manufacturers (AIDA).

www.harting.com



Bench-Top Performance In A Pocket-Sized Scope

Pico Technology has released a new range of PicoScope 2000 Series oscilloscopes that are as small as a passport with a thickness of only 19mm. Connected to and powered from a USB port, they offer bandwidths up to 200MHz and feature an arbitrary waveform generator, yet are almost 80% smaller than the previous generation of PicoScopes. This makes them the perfect scopes for engineers on the move to keep in their laptop bag, while offering all the features and performance of a traditional bench-top oscilloscope.

The specifications include a maximum sampling rate of 1GS/s, adjustable analogue offset over the full input range and high-speed USB streaming up to 1MS/s for waveform captures of up to 100 million samples in length. The built-in signal source can act as a standard signal generator (sine, square, triangle and others) with programmable sweep or as a 12-bit 20MS/s full-function arbitrary waveform generator.

www.picotech.com



YOKOGAWA'S ADDS NEW SCOPECORDERS TO ITS PRODUCT FAMILY

Yokogawa has added two new instruments to its ScopeCorder family of portable multi-channel data-acquisition recorders. The new DL850E and DL850EV (Vehicle Edition) ScopeCorders incorporate a number of new features to allow engineers to measure and analyse a wealth of signals in real time and to speed up development and fault finding in areas such as power electronics, mechatronics and transportation.

In addition to the high-speed multi-channel capabilities plus long memory and isolated input channels found in Yokogawa's established ScopeCorder family, the new DL850E instruments carry out the real-time measurement and analysis of electrical power.



All members of the ScopeCorder family are equipped with a set of basic arithmetic mathematical functions, but the new DL850E versions also offer the /G5 option for real-time measurement of electrical power, as well as the existing /G3 option for real-time mathematical computations and digital filtering and the /G2 option for user-defined computations.

www.tmi.yokogawa.com

Linear Current-Sensor IC Is Thermally Enhanced For High Precision

The new ACS770 from Allegro MicroSystems Europe is a fully integrated Hall-effect based linear current sensor IC incorporating thermal enhancement for high precision.

The new device consists of a precision, low-offset linear Hall circuit with a copper conduction path located near the die. Applied current flowing through this copper conduction path generates a magnetic field which the Hall IC converts into a proportional voltage.

The industry-leading total output accuracy of the ACS770 is achieved by using a new piecewise linear digital temperature compensation technique for offset and sensitivity. This greatly improves the IC's accuracy and temperature stability without influencing the high-bandwidth (125kHz) operation of the analogue output. Outstanding noise

performance results from the use of proprietary amplifier and filter design techniques.

Device accuracy is optimised through the close proximity of the magnetic signal to the Hall transducer. Low power loss results from the fact that the internal resistance of this conductive path is typically only 100 microhms.

www.allegromicro.com



PIC32MZ 32-BIT MCUS LAUNCHED, OFFERING CLASS-LEADING PERFORMANCE

Microchip has announced the new 24-member PIC32MZ Embedded Connectivity (EC) family of 32-bit MCUs. It provides class-leading performance of 330DMIPS and 3.28CoreMarks/MHz, in addition to dual-panel, live-update Flash (up to 2MB), large RAM (512KB) and connectivity peripherals – including a 10/100 Ethernet MAC, Hi-Speed USB MAC/PHY (a first for PIC MCUs) and dual CAN ports – needed to support today's demanding applications.

The PIC32MZ also has class-leading code density that is 30% better than competitors, along with a 28MSPS ADC that offers one of the best throughput rates for 32-bit MCUs.

Completing this family's high level of integration is a full-featured hardware crypto engine with a random number generator for high-throughput data encryption/decryption and authentication

such as AES, 3DES, SHA, MD5 and HMAC, as well as the first SQL interface on a Microchip MCU and the PIC32's highest number of serial channels.

In addition, Microchip announced the industry's most comprehensive 32-bit microcontroller firmware development framework called MPLAB Harmony.

www.microchip.com



Combined EMC Antenna And Pre-Amplifier Pairs For Enhanced Measurement Integrity

ETS-Lindgren has announced a significant improvement in antenna measurement integrity when using the company's EMC antennas. Combined EMC antenna and matched pre-amplifier pairs are now available with antenna factors which take account of the characteristics of both antenna and amplifier. System calibration is now provided with each shipment.

ETS-Lindgren announced that its popular Double-Ridged Waveguide Horn and BiConiLog antennas are now available together with matched pre-amplifiers. Known as Models 3116C-PA and 3117-PA, the antenna and pre-amplifier combination are calibrated as a single unit. This allows for mismatches between the antenna and the pre-amplifier to be taken into account in the antenna factor (AF) which is provided with each unit.

Key characteristics of each antenna include single lobe radiation, extremely low AF and flexible mounting. Model 3116C-PA is ideal as a receive antenna for emissions testing from 18GHz to 40GHz. Model 3117-PA is used as a receive antenna for emissions testing from 1GHz to 18GHz.

www.ets-lindgren.com



HIGH CURRENT AXIAL FILTER CHOKES NOW AVAILABLE FROM TFC

Now available from Total Frequency Control Ltd (TFC) is type DRH high current filter chokes, with a wide range of inductance and high saturation current. Ideal for use in switching regulated power supply applications, low profile and self-leading, the finished product is varnish coated or insulated with UL shrink-sleeving. The inductors also feature a useful central hole to facilitate automatic mechanical mounting.

This product is ideally suited in applications such as power supplies and power amplifiers, switching regulators, speaker crossover networks and RFI suppression. Power density dictates the dimensions which vary from 3-5mm in height and 21-28mm in diameter.

Inductance ranges from 1µH up to 15mH with maximum current density of 8.0A/mm² over an operating temperature of -20°C to 80°C. The product exhibits low DCR values and high saturation currents.

TFC manufacturing includes high precision quartz products for resonators, qcm, material lapping and polishing, precision OCXO, TCXO and VCXO oscillators and frequency standards.

www.tfc.co.uk



ATTRACTIVE ENTRY PRICE FOR COM EXPRESS WITH QUAD-CORE INTEL CELERON PROCESSOR

congatec AG, a manufacturer of embedded computer modules, has released the conga-TCA3 COM Express module, available in seven variants based on the new Intel Atom processors E3800 product family and Intel Celeron processor N2920 (formerly codenamed "Bay Trail").

The COM Express Type 6 compact (95 x 95mm) module offers a compelling entry price for this form factor, and the Intel Celeron N2920 1.6GHz quad-core variant features a stunning scenario design power (SDP) of only 4.5W. SDP provides realistic information on average power consumption in practice. Innovations include a large L2 cache shared by multiple cores and a faster Intel HD graphics unit compared with the previous generation. This turns new applications into visual experiences.

The modules support Intel Advanced Encryption Standard New Instructions (Intel AES-NI) set, which is more relevant than ever in practical application. This allows developers to offload particularly compute-intensive packaging and encryption routines of the well-known cryptographic algorithm AES (Advanced Encryption Standard) into hardware.

www.congatec.com

NEWLY DESIGNED OCXO FROM IQD DELIVERS CLASS LEADING ULTRA LOW PHASE NOISE PERFORMANCE

IQD's new IQOV-200F OCXO delivers exceptional phase noise performance with a close-in measurement of -130dBc @100Hz and a noise floor better than -180dBc across a high frequency range of 80-130MHz.

Phase noise is the term used to quantify signal noise in the frequency domain and such phase noise measurements and specification limits are common to most RF engineers in their work. In the time domain, signal purity is described in terms of jitter so measurements and specification limits on jitter are common to digital signal engineers. Combining the high performance expected from an IQD SC-cut crystal based OCXO, the IQOV-200F delivers a frequency stability of ±50ppb over the standard -20 degC to 70degC operating temperature range. Housed in a 36 x 27mm 'Eurostyle' package and running off a 12V supply, it offers a sinewave output of 13dBm min. Furthermore, the IQOV-200F offers comparatively low power consumption of just 150mA max at 25 degrees C and 350mA max during warm up.

www.iqdfrequencyproducts.com



TEKTRONIX BRINGS 165 MHZ REAL-TIME BANDWIDTH TO MID-RANGE SPECTRUM ANALYZERS

Tektronix announced that its real-time spectrum analyzers (RTSAs) now offer up to 165MHz acquisition bandwidth, the widest available in this price range. This bandwidth supports demanding applications such as high-margin, high accuracy WLAN 802.11ac characterization and troubleshooting.

Also improved are the real-time performance and signal detection in the RSA5000 and SPECMON series of RTSAs, further establishing them as premier spectrum analyzers, and the value leaders in their price segments.

Tektronix RTSAs offer unique features that include density trigger, time-qualified triggers and innovative swept DPX display technology that makes it easier to find unwanted transmissions. These instruments also offer the industry's best integration of real-time and multiple domain analysis, with all interactions available through a single interface. Key features include up to 165MHz acquisition bandwidth; a 33% improvement of the minimum signal duration for 100% Probability of Intercept (POI), at a class-leading 2.8µsec; highest performance real-time features, previously available for an extra cost and others.

www.tektronix.com



Custom Temperature Sensors from ATC Semitec

ATC Semitec supplies custom temperature sensors using NTC and PTC thermistors, platinum resistance (Pt100/Pt500/Pt1000) or non-contact, infra-red sensing thermopile technology.

Cost-effective IP68 rated sensors ensure absolute moisture integrity in ground water or refrigeration applications, whilst fast response versions can react in under one second to temperature changes. The wide range of gas boiler temperature sensors provides fast and accurate water temperature control to help provide a comfortable living environment.

ATC Semitec's platinum sensors happily control processes up to 500degC and offer long-term stability. Thermopile sensors can react in milliseconds to infra-red energy changes in non-contact applications, both industrial and medical.

For further information contact ATC Semitec to discuss your latest temperature sensor application.

www.atcsemitec.co.uk



Lattice Announces HetNet Solutions Portfolio Of Programmable Solutions

Lattice Semiconductor announced a portfolio of programmable solutions for building smart, low-power cellular equipment needed to support the global rollout of Heterogeneous Networks (HetNet). In collaboration with Azcom Technology, the Lattice HetNet solutions portfolio enables system designers to implement best-in-class solutions for connectivity, control path and power

management while accelerating their development with system-level reference designs for multi-mode LTE small cells.

Service providers around the world are deploying a mosaic of wireless equipment in both indoor and outdoor environments, including office buildings, public facilities and underground areas to support the explosive growth in mobile data traffic. According to the Small Cell Forum, the small cell market alone is expected to generate \$22bn by 2016.

The Lattice HetNet solutions portfolio enables designers of small cells, low-power remote radio heads, distributed antenna systems and active antennas, to achieve the lowest BOM, power consumption and smallest footprint for the connectivity, control path and power management functions of their systems.

www.latticesemi.com

EXTENDED RANGE OF RFI/EMI SMD SPRING CONTACTS THAT SAVE SPACE AND COST

Harwin has expanded its range of EZ-Spring Contacts with different contact styles and heights. Part of the EZ-BoardWare range of PCB hardware products, the surface mount Spring Contacts – also known as Spring Fingers or Grounding Contacts – are now available in 15 different sizes, ranging from 1.7mm to 7.25mm free height (1.20mm to 6.35mm minimum working height), and are suitable for both vertical and horizontal contact actions.

Designed for easy assembly onto PCBs, EZ-Spring Contacts are used as grounding or shielding contacts in contact with metal frames or shields, or even for general electrical connection between PCBs or similar. Mounted in a row, the contacts can provide an excellent RFI shielding connection for metal doors or other cabinet enclosures. The contact design ensures positive contact with the mating surface and is tolerant to both wiping and sliding action.

Individual clips are supplied in tape and reel packaging for automated placement.

www.harwin.co.uk



300mA LDO REGULATORS WITH LOW QUIESCENT CURRENT

Advanced Power Electronics Corp (USA), a Taiwanese manufacturer of MOS power semiconductors and ICs for DC-DC power conversion applications, has announced a new series of low drop-out linear regulators that include current and thermal shutdown protection features. APE8800A-HF-3 positive linear regulators have a very low quiescent current of about 30µA, an output voltage accuracy of ±2% and can supply a guaranteed 300mA of output current with a drop-out voltage of only 250mV.

APE8800A-HF-3 regulators are able to operate with low ESR ceramic output capacitors as small as 1µF for stability. As well as current limit protection, the APE8800A-HF-3 also offers an on-chip thermal shutdown feature providing protection against overload or conditions where the junction temperature may exceed the specified thermal shutdown temperature.

The new regulators are available with several fixed output voltages from 1.2V to 5V and are packaged in low-profile, space-saving RoHS/REACH-compliant halogen-free 5-lead SOT-23-5 and TSOT-23-5 packages.

www.a-powerusa.com



AVX AND WALDOM ELECTRONICS IN STRATEGIC ALLIANCE

AVX has entered into an alliance with Waldom Electronics over its portfolio of tantalum, ceramic, film and niobium oxide capacitors being offered to this master distributor's network of regional distributors who have local presence, but not the authorization to be a distributor. Waldom will also offer support for stock-outs, extended EOLs, new product introductions and engineering kits designed to facilitate the design-ins of AVX products.

"By providing preferred pricing, broken pack quantities, low minimum order quantities, off-the-shelf delivery and custom kitting specifically tailored to the unique needs of many distributors, Waldom is helping AVX supply our best-in-class components to an even broader segment of this key sales channel," said Pete Venuto, AVX Vice President of Sales.

"Working with premier suppliers like AVX is precisely the type of strategy that has earned Waldom Electronics its reputation as the recognized leader in the billion-dollar electronic component redistribution market," said Waldom Electronics's Corporation General Manager, Robert Derringer.

www.avx.com

World's First Inductance-to-Digital Converter from TI in Stock at Mouser

Mouser Electronics is now stocking the world's first inductance-to-digital converter from Texas Instruments (TI) which is a contactless, short-range sensing technology at low cost.

The TI LDC1000 inductance-to-digital converter provides a sensing technology that offers high-resolution sensing of conductive targets in the presence of dust, dirt, oil and moisture, making it extremely reliable in hostile environments. Using a coil which can be created on a PCB as a sensing element, the LDC1000 enables ultra-low cost system solutions. Inductive sensing technology enables precise measurement of linear/angular position, displacement, motion, compression, vibration, metal composition, ideal for applications in markets such as automotive, consumer, computer, industrial, medical and communications.

The LDC1000 is the world's first inductance-to-digital converter, offering the benefits of inductive sensing in a low-power, small-footprint solution. The product is available in a SON-16 package and offers several modes of operation. An SPI interface simplifies connection to an MCU.

www.mouser.com



Sulphur-Resistant Chip Resistors From Yageo Available From TTI Inc

Yageo's expanded AF series of sulfur-resistant chip resistors can now be ordered from TTI, Inc. The recently introduced 4-pin, 2-resistor (0402 x 2) AF122 arrays and 8-pin, 4-resistor (0402 x 4) AF124 arrays help meet increased market demands. Offering a stable and reliable performance in a wide variety of environments, including those with high level of sulfur, AF arrays save space on the PCB and save time in pick and place applications. To improve the sulfur resistant capability, Yageo utilizes a special material in the inner electrode with the alteration of the resistor structure.

AF series chip resistors meet the requirements of the ASTM-B-809-95 standard, 60degC, 1,000hrs. The devices provide high stability and reliability in harsh environments and are ideal for use in applications such as mining, communication base stations, industrial equipment controls, power supplies, computing servers, consumer electronics and DRAM modules among others.

www.ttieurope.com



Digital Oscilloscope

DS1000E Series



2 Channels
50-100MHz BW
1GSa/s Sample Rate
USB

From £219 + VAT

TELONIC
www.telonic.co.uk
Tel : 01189 786 911

RIGOL
WWW.RIGOL-UK.CO.UK

Apacer

THE MOST RELIABLE STORAGE FOR INDUSTRIES

Industrial MEMORY SOLUTIONS



www.apacer.com

Industrial SSD SOLUTIONS



embedded@apacer.nl

New Handle Version Schroff RatiopacPRO Case

User-friendliness is always the focus of Pentair's electronics packaging products. For this reason a new handle version has been developed for the Schroff RatiopacPRO case with a dual function. This new carrying handle with built-in 19" bracket allows cases containing electronics to be safely handled as well as being securely mounted in an electronics cabinet using the 19" bracket.

The new type of handle is a cast element and its design is based on familiar handle types. The depth of the handle is such that this version can also be used in cabinets with a door. Its carrying capacity and robustness have been verified with load tests with roughly 1,000,000 cycles and a weight of 25kg. This handle version is available in the sizes 2U, 3U, 4U and 6U for RatiopacPRO and in sizes 3/4U and 6/7U for RatiopacPRO air. Existing RatiopacPRO cases with ordinary handles or 19" brackets can also be modified to the new combined handle version.

www.schroff.co.uk/ratiopacpro



Telephone: 01840-770028
Fax: 01840-770705
7 Gavercoombe Park Tintagel, Cornwall PL34 0DS
www.kestrel-electronics.co.uk

KESTREL
Electronic Components Limited

100+ PRICES
many other PICS available

PIC16C711-04/P	1.18	PIC16F887-I/P	1.18
PIC16C711-04/SO	1.05	PIC16F887-I/PT	1.16
PIC16F737-I/SP	2.01	PIC16F1823-I/P	0.68
PIC16F818-I/P	0.99	PIC16F1824-I/SL	0.51
PIC16F818-I/SO	0.94	PIC16F1827-I/SO	0.62
PIC16F819-I/P	0.99	PIC16F1828-I/SS	0.55
PIC16F819-I/SO	1.12	PIC16F1829-I/SS	0.63
PIC16F870-I/SP	1.68	PIC16F1847-I/SO	0.71
PIC16F873A-I/SP	2.15	PIC16F1933-I/SS	0.71
PIC16F873A-I/SO	1.99	PIC16F1939-I/PT	1.21
PIC16F874A-I/P	2.28	PIC18F45K22-I/PT	1.25
PIC16F876A-I/SP	2.25	PIC18F252-I/SP	3.05
PIC16F876A-I/SO	2.25	PIC18F442-I/P	3.21
PIC16F877A-I/P	2.35	PIC18F452-I/P	3.35
PIC16F877A-I/PT	2.76	PIC18F458-I/PT	3.59
PIC16F882-I/SS	0.89	PIC18F2420-I/SP	2.04
PIC16F883-I/SP	1.02	M27C4001-10F1	2.75
PIC16F883-I/SO	0.82	M27C2001-10F1	2.81
PIC16F884-I/P	1.05	M27C1001-10F1	2.44
PIC16F886-I/SP	1.09	M27C512-10F1	1.95
PIC16F886-I/SO	0.91	M27C256B-10F1	1.75

We can also supply Maxim/Dallas, Lattice, Linear Tech
PLEASE VISIT OUR WEB SITE FOR FULL LIST

TELONIC **KIKUSUI**
www.telonic.co.uk info@telonic.co.uk



AC POWER SUPPLIES /
FREQUENCY CONVERTERS



DC ELECTRONIC LOADS



ELECTRICAL SAFETY TESTERS



PROFESSIONAL DC POWER
SUPPLIES

Tel : 01189 786 911 Fax : 01189 792 338

TELONIC
www.telonic.co.uk

PROGRAMMABLE DC POWER SUPPLIES 2 - 900kW



MAGNA-POWER ELECTRONICS

Tel: 01189786911 • Fax: 01189792338
www.telonic.co.uk • info@telonic.co.uk

SOUTH KOREAN PRESIDENT PROMOTES INTERNATIONAL ENERGY COOPERATION

The South Korean President Park Geun-hye told energy leaders at the World Energy Congress in Daegu recently that international cooperation is needed to meet global energy challenges, while a “creative energy economy” should be promoted in which Korea can play a leading role.

“The Energy Trilemma, the trade-offs between energy security, social equity and environmental impact mitigation, is the most significant challenge,” she said in the Congress keynote address.

In response, increased global energy cooperation is needed, particularly between energy producing and consuming countries, which would contribute to global market stability. President Park said such cooperation was important for Asia, which has a mix of countries that are either heavy energy consumers or have large energy reserves.

In addition, the world must switch from a traditional energy economic model to a creative energy economy, which would promote energy conservation and environmental production through the use of smart grids, LEDs and low-emission vehicles. But to achieve this goal, the private sector needs to play an important financing role when governments face budget problems, said President Park.

Economies need to adopt energy policies that would deliver “clean, safe and available energy for all,” she continued. Measures should include revising energy price frameworks and regulations to promote energy efficiency, a more equitable distribution of energy resources, as well as encouraging investment in clean energy technology.

Energy experts set the energy trilemma in the context of challenges that are expected to persist through the coming decades.

Maria Van der Hoeven, Executive Director of the International Energy Agency (IEA) said: “Energy efficiency is at the heart of any solution for Europe and for our energy trilemma.”

Luis Enrique Berrizbeitia, Executive Vice President of the Development Bank of Latin America (CAF), also advocated an integrated approach, drawing on the experience of Latin America. “There are plenty of opportunities to satisfy security needs, especially if we make progress on the integration front,” he said. “Integration can combine all of the region’s resources in an efficient manner.”

new industrial revolution, giving concrete answers to the need for employment and the improvement in the quality of life.

Efforts must be made for the world to cooperate on energy, because at present there’s a great rich/poor imbalance, which in consequence increases poverty, diseases and pollution.

In my opinion, the world’s energy cooperation requires a good policy to prepare for the future after oil. It is necessary to strengthen energy cooperation between neighbouring countries and on an international scale. In addition, it is necessary that the European countries, the United States, China and Japan strengthen their energy cooperation as world leaders. For this cooperation to succeed it is necessary to provide a mechanism of international dialogue which will strengthen their exchanges and cooperation in the fields relating to oil, natural gas, coal, electricity and renewable energies. They must reciprocally engage with each other for their mutual benefit and that of the rest of the world. They need to cooperate regarding exploitation of resources and to stabilize the prices of around energy-generating products. To live in this world full of changes, it is time to join forces for a better future.

PROFESSOR DR DOGAN IBRAHIM, Near East University in Nicosia, Cyprus: With the growing world population and the fast advances in technology, the demand for energy is at an all-time peak. I welcome the proposals of President Park Geun-hye calling on world leaders to cooperate to create worldwide energy policies where all nations can benefit and, in particular, policies should be created for the efficient use of energy worldwide.

It is encouraging to hear that South Korea wishes to play a leading role in this cooperation.

BARRY MCKEOWN, RF and Microwave Engineer in the Defence Industry, and Director of Datod Ltd, UK: It is said that tomorrow never comes; unfortunately it does, with monotonous regularity, so shall we face a Trilemma? Defined as a difficult choice between three options? Nope – this is the usual economist forecasting nonsense and should not be confused with real global warming issues.

The fact that it just relates to current issues concerning EM energy means that as engineers and scientists we should not fall for it. Witness the recent advances in data centre energy requirements, whereby 55% of these centres are, in fact, counter-intuitively, actually utilising less power now than they were five years ago.

When the transistor was invented by John Bardeen, Walter Brattain and William Shockley in 1947, it revolutionized the field of electronics. In March this year a team of bioengineers from Stanford University led by Drew Endy announced the creation of a biological equivalent of the transistor, which they named a “transcriptor”. Just as in 1947 no-one could predict the implications for the technology today, thus no-one can predict the consequences of the energy requirements of transcriptor-based technologies and what they will evolve into, and the same is true with quantum computers. But, I can safely predict that it won’t be an economist who sorts out these issues but tomorrow’s scientists and engineers.

MAURIZIO DI PAOLO EMILIO, Ph.D and Engineer - University of L’Aquila/INFN, Italy: The themes of change will continue well into the middle of this century. The future for the leaders of our industry is going to demand thinking more broadly about the purpose of our business, about the nexus of energy with other critical resources, and about new and innovative collaborations for solving critical societal challenges.

The rise of China and India, along with other emerging economies, also has important implications for the architecture of global energy cooperation. It is appropriate to assess the impact the newcomers have on existing forms of cooperation and to examine how these need to adjust to ensure effectiveness.

HAFIDH MECHERGUI, Associate Professor in Electrical Engineering and Instrumentation, University of Tunisia: The price of energy continues to increase and many countries in the world suffer in the process. In addition, the environmental and health damage continue and climatic disorders accelerate.

More than ever our future depends on energy. The World Energy Congress has raised important points for the future of energy cooperation. Indeed, such an initiative becomes a need nowadays; it is a chance to open the prospects for the future of humanity. Such cooperation must be founded on energy saving. It would be the lever of a

CAD CONNECTED



PROTEUS DESIGN SUITE VERSION 8

Featuring a brand new application framework, common parts database, live netlist and 3D visualisation, a built in debugging environment and a WYSIWYG Bill of Materials module, Proteus 8 is our most integrated and easy to use design system ever. Other features include:

- Hardware Accelerated Performance.
- Unique Thru-View™ Board Transparency.
- Over 35k Schematic & PCB library parts.
- Integrated Shape Based Auto-router.
- Flexible Design Rule Management.
- Polygonal and Split Power Plane Support.
- Board Autoplacement & Gateswap Optimiser.
- Direct CAD/CAM, ODB++, IDF & PDF Output.
- Integrated 3D Viewer with 3DS and DXF export.
- Mixed Mode SPICE Simulation Engine.
- Co-Simulation of PIC, AVR, 8051 and ARM MCUs.
- Direct Technical Support at no additional cost.

**Version 8.1 has now been released
with a host of additional exciting new features.**

For more information visit.

www.labcenter.com

***When you really DO need
your mobile phone to
have battery power!***

***STAY IN COMMUNICATION WITH
POWER ON THE GO FROM
POWERSOLVE PORTABLE MOBILE
POWER BANK CHARGERS***



Compatible with all mobile phones and electronic devices such as tablet PC's, iPads, digital cameras, in fact anything supported by 5V USB charging technology

The model **PAF10AH4** shown here has powerful lithium batteries that would charge a typical smart phone 5 times from one single charge. Ideal for camping, fishing, etc., etc.

IDEAL UNIQUE GIFT FOR CHRISTMAS!



***Buy online now
while stocks last!
Lots of models
including solar
chargers
Prices start from
£25.95 each***

www.powersolvemobile.com

**POWER
SOLVE**